行政院國家科學委員會專題研究計畫 成果報告

綠色建築三合一整合光伏電熱太陽能板(PV/T)空氣收集器，地熱空氣交換器(EAHE)及鋪設穩態形狀相變材料地板(SSPCM)的能量與最大可用能之分析研究

研究成果報告(精簡版)

計 畫 類 別 ：個別型
計 畫 編 號 ：NSC 99-2221-E-216-030-
執 行 期 間 ：99 年 08 月 01 日至 100 年 07 月 31 日
執 行 單 位 ：中華大學機械工程學系

計 畫 主 持 人：蔡博章

計畫參與人員：碩士班研究生-兼任助理人員：張宇志
碩士班研究生-兼任助理人員：賴世傑

報 告 附 件 ：出席國際會議研究心得報告及發表論文

公 開 資 訊 ：本計畫涉及專利或其他智慧財產權，2 年後可公開查詢

中 華 民 國 100 年 10 月 31 日

中文摘要： 建築物越來越注重本身自己就是節能減碳有效率，因此自然通風、太陽能加溫與致冷、地溫空氣熱交換、自然光線及避陽遮蔭…等自然被動式不需要消耗太多能量的設置，將是綠色建築的不二選擇，本研究三機一體將薄膜光伏電熱太陽能板空氣收集器(PV/T aircollector), 收集熱氣驅動氣流、搭配地溫空氣熱交換(EAHE)來的氣流與吸收透過窗戶或太陽能板光線的穩態形狀相變材料地板(SSPCM)之儲熱儲能，利用新設計分階相變活塞氣缸壓氣機作系統氣流、溫度的自然調配，整合出一棟完全被動式混成系統建築。考慮新材料與建築服務結合的綠色設計新觀念，再以一棟位於台灣新竹地區沒有空調的建物為探討對象，來數值分析仲夏夜晚通風情況下，氣、電及熱的需求與影響，分析時程含蓋日、月及年，先針對薄膜光伏電熱太陽能板與各次系統之物理數學模型(Model)驗證，再發展出被動式混成系統建築的完整物理數學模型，搭配 MATHLAB、CFD 軟體協助而得到分析解及數值解。致於現在正在進行利用熵值公式(enthalpy formulation)及 Voller 與 Patankar 之控制容積數值技術求解二維暫態能量守恆搭配 Stefan 移動邊界問題之福傳程式組 Hybrid-HVAC，也將配合本棟被動式混成系統建築的個別次系統做程式修改為 Hybrid-HVACP，此程式可以幫忙材料作驗證，以及協助太陽能電池空氣收集器、地溫空氣熱交換及穩態形狀相變材料地板等系統作設計，為綠色建築-節能省能屋的最佳化設計與能量分析，提供有利的工具。
本研究將花費一年時間發展，以 2010 年 8 月 1 日到 31 日 0am-24pm 及 2011 年各個月新竹市的氣象資料當樣本，設定系統與次系統參數到本樣品屋，進行可行性評估、加溫與致冷能力分析、空調性能、次系統操作條件改變時如空氣流量改變，環境溫度與室內溫度的變化及隨氣候分級環境溫度變化時，本被動式混成系統建築的逐月逐年的能量分析…等，希望本研究成果能協助居民對各式各樣節能省能技術作選擇，並促成人們有健康、舒適地居住環境的美夢能成真。

英文摘要： The self-sufficiency of buildings is becoming increasingly important. Therefore, devices for natural ventilation, solar heating and cooling, ground cooling (earth- air heat exchangers), natural lighting, shading from the sun, and other devices that use a passive mode strategy have been developed. Sustainability-oriented choices that might in the pass have been considered to be optional are now necessary. In this work, thin film photovoltaic technology is utilized in buildings. An integrated photovoltaic /thermal (PV/T) air collector to collect hot air and drive air flow, and mixing the air flow from earth-air heat exchanger (EAHE) and hot air flow to the floor that is made of shape-stabilized phase change material (SSPCM) floor inside greenhouse, a SSPCM absorbs energy form

solar light that enters through windows and solar panels. A piston cylinder air compressor adjusts the moderate control of air flow and the ambient temperature and temperature of room in the hybrid system. The hybrid system using natural ventilation in passive strategies designs an innovative HVAC system can be called ’lung’ of a building. The design process integrated with ‘‘whole building approach’ and ‘‘new material’ is used to analyze the theoretical performance of this building by energetic analyses for the weather in HsinChu. A mathematic model will be resolved by the helps of MATLAB 7.0 program and CFD software. The energy required by air-conditioning and thermal will be predicted. A finite difference-Fortran program (Hybrid-HVAC) is developed based upon the 2D unsteady heat equation with a Stefan moving boundary problem. This program is modified into a Hybrid-HVACP and should enable the hybrid system building with the PV/T、EAHE and SSPCM to be solved numerically with high accuracy. The simulation results in this work reveal that if the difference between ground temperature and ambient temperature is less than 5 K, such as in HsinChu city, the HVAC results obtained using EAHE are unsatisfactory, and so EAHE yields better results in areas with large temperature differences.

附件一

行政院國家科學委員會補助專題研究計畫 ■ 成 果 報 告 □期中進度報告

綠色建築三合一整合光伏電熱太陽能板(PV/T)空氣收集器, 地熱空氣交換器(EAHE)及鋪設穩態形狀相變材料地板(SSPCM)的能量與最大可用能之分析研究

計畫類別：■個別型計畫　　□整合型計畫

計畫編號：NSC－99－2221－ E －216－030

執行期間： 99 年 08 月 01 日至 100 年 07 月 31 日

執行機構及系所：中華大學機械工程學系

計畫主持人：蔡博章

共同主持人：

計畫參與人員：張宇志、賴世傑

成果報告類型(依經費核定清單規定繳交)：■精簡報告　□完整報告

本計畫除繳交成果報告外，另須繳交以下出國心得報告：

□赴國外出差或研習心得報告

□赴大陸地區出差或研習心得報告

■出席國際學術會議心得報告

□國際合作研究計畫國外研究報告

處理方式：除列管計畫及下列情形者外，得立即公開查詢

□涉及專利或其他智慧財產權，□一年■二年後可公開查詢

中　華　民　國 100 年 10 月 26 日

目錄:

Theoretical performance of integrated photovoltaic /thermal air collector, earth-air heat exchanger and greenhouse with a floor of shape-stabilized phase-change material: evaluation by energetic analyses

蔡博章[1]、張宇志[2]、賴世傑[3]
[1]中華大學機械工程研究所教授
[2,3]中華大學機械工程研究所研究生
國科會計畫編號. : NSC 99-2221-E-216-030

Abstract

The self-sufficiency of buildings is becoming increasingly important. Therefore, devices for natural ventilation, solar heating and cooling, ground cooling (earth- air heat exchangers), natural lighting, shading from the sun, and other devices that use a passive mode strategy have been developed. Sustainability-oriented choices that might in the pass have been considered to be optional are now necessary. In this work, thin film photovoltaic technology is utilized in buildings. An integrated photovoltaic /thermal (PV/T) air collector to collect hot air and drive air flow, and mixing the air flow from earth-air heat exchanger (EAHE) and hot air flow to the floor that is made of shape-stabilized phase change material (SSPCM) floor inside greenhouse, a SSPCM absorbs energy form solar light that enters through windows and solar panels. A piston cylinder air compressor adjusts the moderate control of air flow and the ambient temperature and temperature of room in the hybrid system. The hybrid system using natural ventilation in passive strategies designs an innovative HVAC system can be called "lung" of a building. The design process integrated with "whole building approach" and "new material" is used to analyze the theoretical performance of this building by energetic analyses for the weather in HsinChu. A mathematic model will be resolved by the helps of MATLAB 7.0 program and CFD software. The energy required by air-conditioning and thermal will be predicted. A finite difference-Fortran program (Hybrid-HVAC) is developed based upon the 2D unsteady heat equation with a Stefan moving boundary problem. This program is modified into a Hybrid-HVACP and should enable the hybrid system building with the PV/T、EAHE and SSPCM to be solved numerically with high accuracy. The simulation results in this work reveal that if the difference between ground temperature and ambient temperature is less than 5 K, such as in HsinChu city, the HVAC results obtained using EAHE are unsatisfactory, and so EAHE yields better results in areas with large temperature differences.

Keywords: Photovoltaic/thermal air collector, Earth air heat exchanger, Shape-stabilized phase change material, HVAC, Solar energy.

I. Introduction

In Europe, almost half (about 40%) of all power consumed is associated with buildings, especially in their construction and maintenance, but mostly in their operation. Therefore, an increasing attention is being paid to the self-sufficiency of buildings, as demonstrated by the new European (and national) regulations concerning the energetic certification of buildings. Sustainability-oriented choices that could have been considered optional previously are now necessary. Therefore, energy is no longer something of interest only to researchers, but is now a "new consideration" in the design processes of architects and engineers.

This investigation concerns the weather in HsinChu city [1], and the application of thin film photovoltaic technology in buildings. An integrated photovoltaic/thermal (PV/T) air collector for collecting hot air and driving air flow mixes the air flow from the earth-air heat exchanger (EAHE). Hot air flows to the floor that is made of shape-stabilized phase change material (SSPCM) floor inside greenhouse. SSPCM absorbs energy form solar light that enters through windows and solar panels. A piston cylinder air compressor adjusts moderate air flow and ambient and room temperatures in the hybrid system. The hybrid system using natural ventilation in passive strategies designs an innovative HVAC system can be called "lung" of a building.

The literature on the PV/T integrated hybrid system is surveyed. Chow [2] analyzed the performance of a photovoltaic-thermal collector by using an explicit dynamic model and found a thermal efficiency of 60%. Arrangements for utilizing thermal energy as well as electrical energy that include a photovoltaic module are referred to as the hybrid PV/T systems. The thermal energy that is obtained from the hybrid photovoltaic (PV/T) system is supplied to the greenhouse for heating. Tiwari and Sodha [3] examined the thermal performance of a hybrid with photovoltaic/thermal (PV/T) air collector. Nayak and Tiwari [4] studied the performance evaluation of a hybrid photovoltaic/thermal (PV/T) integrated greenhouse system. They obtained a thermal efficiency of the hybrid photovoltaic/thermal (PV/T) air collector around 34% and a thermal efficiency of the photovoltaic/thermal (PV/T) without airflow is of 8.5%. The thermal efficiency of the PV/T air collector was increased by 25.5% by causing the air to flow. Barnwal and Tiwari [5] investigated the design, construction and testing of a hybrid photovoltaic integrated greenhouse dryer. Dincer [6] studied the energetic performance of heating systems for building in two geothermal districts and found energy efficiencies of heating systems in the Balcova geothermal district and Salihli geothermal district of 39.36% and 59.31%, respectively. Dincer [7] examined the relationships between energy and exergy, energy and sustainable development, energy policy-making, exergy and the environment and exergy. In study of the hybrid system design, and the construction and testing of integrated hybrid photovoltaics, the work of Nayak and Tiwari [8] [9], Dincer [7] is drawn upon to conduct the theoretical analysis and that of Tsai [10] is used to design heat exchanger. The installation of a wall and floor made of the shape-stabilized phase change material (SSPCM) inside building has already studied by the present authors [11-12].

II. PHYSICAL AND MATHEMATICAL ANALYSIS AND MODELING

A rectangular U-shaped EAHE whose bottom is 40m long, 10cm wide and 10cm high and 5m deep, and whose sides are 5m high, 10cm wide and 10cm high on both sides, the thickness of all channel duct surfaces is 10mm. (Fig. 1). The model room (with no roof) is 3.9m long、3.3m wide and 2.7m high. The cement layer is 300mm thick, the layer SSPCM is 100mm thick, the cross sectional area of the air outlet is 100mm x 100mm, and the temperature below 5m below the surface of the ground surface is maintained at 298 K.

1. Energy balance equations for photovoltaic and earth-air heat exchanger integrated greenhouse

The energy balance equations for different components of a greenhouse that is combined with a photovoltaic (PV/T) system and an earth-air heat exchanger (EAHE) are as follows: (Fig. 2)

The term q_U denotes the useful thermal energy that is obtained from a photovoltaic (PV/T) system and Q_u is the useful thermal energy that is obtained from an earth-air heat exchanger (EAHE).

(i) The amount of useful thermal energy obtained hourly form the PV/T system

$$\dot{q}_U = \dot{m}_a c_a (T_{airout} - T_r) = \frac{\dot{m}_a c_a}{U_L}\{h_{p1}h_{p2}(\alpha\tau)_{eff} I(t) - U_L(T_r - T_a)\}\left[1 - e^{(-bU_L/\dot{m}_a c_a)}\right]$$
$$= F_R\{h_{p1}h_{p2}(\alpha\tau)_{eff} I(t) - U_L(T_r - T_a)\} \quad (1)$$

where $F_R = \frac{\dot{m}_a c_a}{U_L}\left[1 - e^{(-bU_L/\dot{m}_a c_a)}\right]$

(ii) The amount of useful thermal energy obtained hourly form the EAHE

$$\dot{Q}_u = F'_R m_a c_a (T_0 - T_r) \quad (2)$$

where $F'_R = 1 - e^{-(2\pi r_1 h_g/\dot{m}_a c_a)L'}$

Combining equations of (i) and (ii) yields the first order partial differential equation:

$$\frac{dT_r}{dt} + aT_r = B(t) \quad , \quad B(t) = \frac{F(t) + (UA)_{eff} T_a}{M_a C_a} \quad ,$$

$$a = \frac{a_1}{M_a C_a} \quad (3)$$

The analytical solution of Eq. (3) can be written as

$$Tr = \frac{\overline{B(t)}}{a}\left(1 - e^{-at}\right) + T_{ro}e^{-at} \quad (4)$$

where T_{ro} is the greenhouse air temperature at t = 0 and B(t)is the average of B(t) for the time interval 0 and t, and a is constant during the time. The rate of daily useful thermal energy obtained from PV/T system:

$$\left(\dot{q}\right)_{daily} = F_R\left\{h_{pi}h_{p2}\left(\alpha\tau\right)_{eff} I\left(t\right) - U_L\Sigma\left(T_r - T_a\right)\right\} \quad (5)$$

$$F_R' = 1 - e^{\left(-2\pi r_1 h_{gf}/\dot{m}_a C_a\right)L'}$$

The rate of daily useful thermal energy obtained from EAHE:

$$\left(\dot{Q}_u\right)_{daily} = F_R' m_a C_a\left[T_0 - T_r\right] \quad (6)$$

And final the total useful thermal energy obtained

$$\left[\left(\dot{Q}_u\right)_{tot}\right]_{daily} = \left(\dot{q}_u\right)_{daily} + \left(\dot{Q}_u\right)_{daily} \quad (7)$$

III. NUMERICAL TECHNIQUE

1. Model room (with or without a roof)

The model room (with no roof) that is used in the analysis is a concrete chamber with dimensions of 3.9 m (length) x 3.3 m (width) x 2.7 m (height). The dimensions of earth-air heat exchanger (EAHE) are given above. (Fig. 3)

2. Input parameters of the model room and applying software

In this study, Gambit was used to construct a solid model and grid mesh, and then Fluent was used to solve the flow and thermal field. Table 1 presents all parameters of the building and material properties of SSPCM. Table 2 presents the conditions of environments outside the model room.

3. Establish grid cells

Fig. 4 presents cells in the grid mesh for this model room (with no roof).

Ground (4662.791 m^3) ：249,885 cells
Concrete layer (113.359 m^3) ： 193,403 cells
SSPCM layer (3.441 m^3) ：136,400 cells
Floor-wood (0.891 m^3) ：7128 cells
EAHE (0.418m^3) ：3352 cells
Air outlet (0.004 m^3) ：32cells

4. Settings of the Fluent

The settings used in the Fluent software are as follows:

1. Solver ：Segregated
2. Space：3D
3. Velocity formulation ：Absolute
4. Gradient option ：Cell-Based
5. Formulation ：Implicit
6. Time ：Unsteady
7. Unsteady formulation ：1^{st}-Order Implicit
8. Porous formulation ：Superficial Velocity
9. Laminar

5. Initial conditions

Energy stored in the cycle is absorbed heat

The ambient temperature and pressure are 303 K and 1atm respectively. The temperature of SSPCM layer is assumed to be at a constant temperature 293 K, the optimal time (i.e. melting/fusing temperature) and its latent capacity is 265MJ/m^3. The initial condition (t=0) of indoor air temperature is 303 K. On the contrary,

Energy released in the cycle is lost heat

The ambient temperature and pressure is 289 K and 1atm respectively. The temperature of SSPCM layer is assumed to be at a constant temperature 303 K, the optimal time (i.e. melting/fusing temperature, and its latent capacity is 265MJ/m^3. The initial condition (t=0) of indoor air temperature is 289 K.

Each time increment $\triangle t$ is 0.1 sec. Iterations are performed up to the specific time until the convergence criteria are satisfied.

The temperature 5m below the ground surface is kept constant at 298K.

6. Boundary conditions

The embedding macro files in the Fluent are used to set the boundary conditions and our case is unsteady. The maximum of solar radiation on the south wall is 900Wm^{-2} and in the HsinChu city, the wind in the summer is southern at 6 ms^{-1} and the average outdoor temperature is 302.96 K, in winter, the wind is southern 6.6 ms^{-1} and the average outdoor temperature is 288.9 K. (Table 2)

7. Convergence criteria

To determine any number of flow field changes in the iterative process, the simulation convergence criteria in Table 3 are imposed.

8. Computational procedure of energy analysis

Equations of the energy balance derived for greenhouse coupled with photovoltaic system and earth air heat exchanger (EAHE), have been solved with the help of a computer program, based on Matlab 7.1 software.

IV. Result and Discussion

A. Simulated temperature results of passive SSPCM

Energy stored in the cycle is absorbed heat

The ambient temperature and pressure are 303 K and 1atm respectively. The temperature of SSPCM layer is assumed to be at a constant temperature 293 K, the optimal temperature (i.e. melting/fusing temperature, and its latent capacity is 265MJ/m^3. The initial condition (t=0) of indoor air temperature is assumed to be 303 K. At this time, initially t = 0, the indoor air temperature exceeds the temperature of the SSPCM layer. Then all SSPCM layers start to absorb heat. Numerical results reveal that as time passes, the average indoor temperature decreases. The average indoor temperature drops from 303 K to 295.93 K within 60 minutes.

SSPCM + EAHE (indoor room temperature around 302.74 K)

In Table 4, the air temperature of EAHE rapidly reaches thermal equilibrium with the ground temperature, and temperature of air that moves from EAHE to the indoor space of the model room remained at around 302.74 K. Little change in air temperature occurs after the heat is exchanged through EAHE. Because the difference between the ambient temperature and the EAHE temperature is small. Figures.5 a-d plot simulated indoor air temperature vs. time (YZ plane at middle X) for the SSPCM + EAHE in an energy stored cycle. Indoor air temperature does not fall but rises at t = 20 minute because SSPCM loses heat more slowly than does the air-out from EAHE, but later at t = 30 minute the indoor air temperature is in thermal equilibrium at 300.52 K.

On the contrary,

Energy released in the cycle is removed heat

The ambient temperature and pressure are 289 K, and 1atm respectively. The temperature of the SSPCM layer is assumed to be at a constant temperature 303 K, the optimal time (i.e. melting/fusing temperature), and its latent capacity is 265MJ/m^3. The initial condition (t=0) of indoor air temperature is assumed to be 289 K. At this time, initially t = 0, the indoor air temperature is smaller than the temperature of the SSPCM layer, subsequently, all SSPCM layers start to release heat. Numerical results reveal that as time passes, the average indoor temperature increases. The average indoor temperature increases from 289 K to 298.8 K within 60 minutes. This process produces heating effect at night time or in the winter.

SSPCM + EAHE (indoor room temperature around 291.35 K)

In Table 5, the air temperature of EAHE rapidly reaches thermal equilibrium with the ground temperature, and the temperature of air from EAHE to the indoor space of the model room remains at around 291.35 K. The air temperature changes only slightly upon after the heat exchange through EAHE, because the ambient temperature and EAHE temperature differ only slightly. Figures 6 a-d plot simulated indoor air temperature vs. time (YZ plane at middle X) for the SSPCM+ EAHE in an energy released cycle. Indoor air temperature does not rise but falls at t = 20 minute because heat is absorbed by SSPCM more slowly than the air-out from EAHE, but later at t = 30 minute the indoor air temperature reaches thermal equilibrium at 294.42 K.

B. Comparison between numerical and analytical results for hourly variation of outdoor air temperature

The above discussions of SSPCM concern idealized cases since the temperature of SSPCM was forced to be constant, therefore latent heat capacity causes melting or fusing in a short period of time, and the temperature difference between the average indoor temperature and indoor air temperature is large around 8 K to 9 K. In fact the average indoor temperature varies sinusoidal cycle with relation to optimal SSPCM temperature. The temperature differences between the average indoor temperature and indoor air temperature in both energy stored cycle and energy released cycle are around 2 K to 4 K. The analytical results have been reported by Xiao [13]. Therefore we can compare our numerical results with each other based upon the hourly variation of outdoor air temperature in HsinChu city on one day in July. (the indoor air temperature is simplified equal to outdoor air temperature). From Fig. 7 indicates that numerical and analytical results are mutually consistent.

C. Results of energy analysis

Eq. (4) has been used for calculating greenhouse air temperature under weather conditions for HsinChu city for the following case:

Photovoltaic is operated and earth air heat exchanger is operated for 24 hr for a typical summer or winter day.

Hourly variation of room air temperature when operated with earth air heat exchanger for 24 hr (with the operation of photovoltaic/thermal system) for a typical summer day is shown in Fig 8. In this case it is seen that room air temperature is around 4－5 K lower than the ambient air temperature at 4 pm, while it is 2－3 K lower at 4 am, due to continuous flow of cold air from earth air heat exchanger to the room.

Hourly variation of room air temperature when operated with earth air heat exchanger for 24 hr (with the operation of photovoltaic/thermal system) for a typical winter day is shown in Fig 9. In this case it is seen that room air temperature is around 3－4 K higher than the ambient air temperature at 1 pm, while it is 5－6 K higher at 5 am, due to continuous flow of hot air from earth air heat exchanger to the room.

Fig. 10 shows the variation of hourly useful thermal energy (MJ) when operated with photovoltaic (PV/T) system and with earth air heat exchanger (EAHE) for a typical summer day. It has been observed that at 12 pm, useful thermal energy is calculated as 16 MJ with the operation of photovoltaic/thermal (PV/T) system, while between 5 and 6 pm, the useful thermal energy decreases due to fall of temperature during evening. And useful thermal energy continuously fall down to 4 MJ while between 3 and 4 am.

Fig. 11 shows the variation of hourly useful thermal energy (MJ) when operated with photovoltaic (PV/T) system and with earth air heat exchanger (EAHE) for a typical winter day. It has been observed that at 12 pm, useful thermal energy is calculated as 16 MJ with the operation of photovoltaic/thermal (PV/T) system, while between 4 and 5 pm, the useful thermal energy decreases due to fall of temperature during evening. It then increases to 14.5 MJ with the operation earth air heat exchanger during night.

V. Conclusions

This study established a close to the actual physical situation in a hybrid system as a whole including sub-systems in this new analysis. The following conclusions are drawn:

(1) The hybrid system’s BIPV、TE、SSPCM heat sink and EAHE efficiency gains can ensure energy-efficiency and cleanness. They can also reduce the CO_2 emissions.

(2) The hybrid system has the low total input power and its use constitutes an active approach to energy-saving.

(3) SSPCM consists of paraffin as dispersed PCM and high-density polyethylene (HDPE) or another material as a supporting material. The total stored energy is comparable with that of traditional PCMs.

(4) SSPCMs of the ceiling and floor can use the same material, temperature range of 297 K to 300 K start energy stored cycle and temperature range of 289 K to 293 K start energy released cycle.

(5) Reducing the temperature difference between the ceiling and the floor to less than 4 K increases the comfortableness of humans.

(6) 297 K is the most comfortable temperature in the HsinChu area.

(7) The simulation results reveal that if the difference between the ground temperature and the ambient temperature is less than 5 K, such as in HsinChu city obtained results are unsatisfactory, so the use of EAHE in areas with a large temperature difference yields better results.

(8) The effect of EAHE is not superimposed on additive with the effect of SSPCM, many parameters need to be considered such as materials, size and operating characteristics, therefore the design optimization is needed.

(9)Working fluid air of EAHE may be replaced with water or refrigerant which has a much larger temperature range than air.

(10) Hourly useful thermal energy (MJ) when operated with photovoltaic (PV/T) system and with earth air heat exchanger (EAHE) for a typical summer day. It has

been observed that at 12 pm, useful thermal energy is calculated as 16 MJ with the operation of photovoltaic/thermal (PV/T) system, then the useful thermal energy decreases due to fall of temperature during evening. And useful thermal energy continuously fall down to 4 MJ while between 3 and 4 am.

(11) hourly useful thermal energy (MJ) when operated with photovoltaic (PV/T) system and with earth air heat exchanger (EAHE) for a typical winter day. It has been observed that at 12 pm, useful thermal energy is calculated as 16 MJ with the operation of photovoltaic/thermal (PV/T) system, while between 4 and 5 pm, the useful thermal energy decreases due to fall of temperature during evening. It then increases to 14.5 MJ with the operation earth air heat exchanger during night.

VI. Acknowledgement

We hereby express our thanks to the National Science Council for the support of research project NSC99-2221-E-216-030.

VII. References

[1] Central Weather Bureau , Taipei, Taiwan: http://www.cwb.gov.tw/ **(2011)**

[2] T.T. Chow, Performance analysis of photovoltaic-thermal collector by explicit dynamic model, Solar Energy 75 (2), 143 **(2003)**

[3] A. Tiwari , M.S. Sodha , Performance evaluation of solar PV/T system: an experimental validation, Solar Energy 80 (7), 751 **(2006)**

[4] S. Nayak, A. Tiwari, Performance evaluation for an integrated photovoltaic/thermal greenhouse system, International Journal for Agricultural Research 2(3), 211 **(2007)**

[5] P. Barnwal, A. Tiwari, Design, construction and testing of hybrid photovoltaic integrated greenhouse dryer, International Journal of Agricultural Research (IJAR)3 (2), 110 **(2008)**

[6] I. Dincer, A. Hepbasli, L. Ozgener, Performance investigation of two geothermal district heating systems for building applications, Energy Analysis, Energy and Buildings 38, 286 **(2006)**

[7] I. Dincer, The role of exergy in energy policy making, Energy Policy 30, 137 **(2002)**

[8] S. Dubey, S.C. Solanki, A. Tiwari, Energy and exergy analysis of PV/T air collectors connected in series , Energy and Building 41, 863 **(2009)**

[9] S. Nayak, A. Tiwari, Theoretical performance assessment of an integrated photovoltaic and earth air heat exchanger greenhouse using energy and exergy analysis methods, Energy and Building 40, 888 **(2009)**

[10] B.J.Tsai, Y.L. Wang, A novel Swiss-Roll recuperator for the microturbine engine, Applied Thermal Engineering 29, 216 **(2009)**

[11] B.J. Tsai, K. Huang and C.H. Lee, Hybrid Structural Systems of an active building envelope system (ABE), Advanced Materials Research, Vols. 168-170, 2359 **(2011)**

[12] B.J. Tsai, S.C. Lin and W.C. Yang, HVAC analysis of a building installed shape-stabilized phase change material plates coupling an active building envelope system. WSEAS Trans. On Heat and Mass Transfer, reviewing, **(2011)**

[13] W. Xiao, X. Wang and Y. Zhang, Analytical optimization of interior PCM for energy storage in a lightweight passive solar room. Applied energy, 86, 2013 **(2009)**

Figures

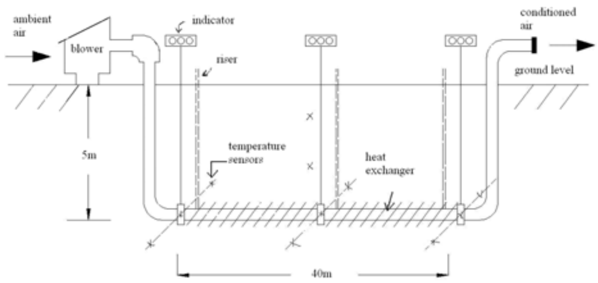

Fig. 1. Earth-air heat exchanger (EAHE)

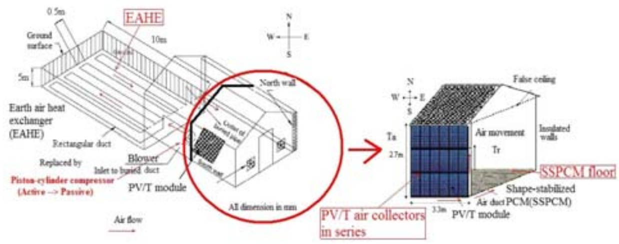

Fig. 2. Self-sufficient building with integrated PV/T, SSPCM and EAHE as well as passive natural ventilation

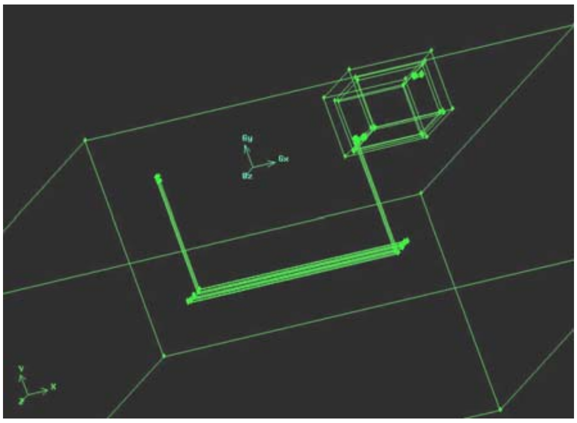

Fig. 3. Model room (without roof) to be analyzed

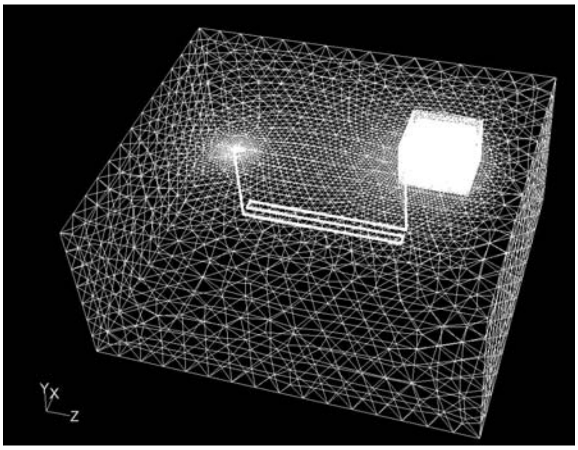

Fig. 4. Grid mesh of the model room and environments

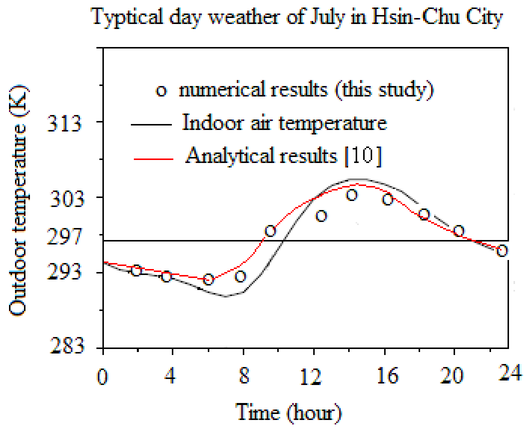

Fig. **7** Twelve-hourly variation of indoor air temperature in HsinChu City

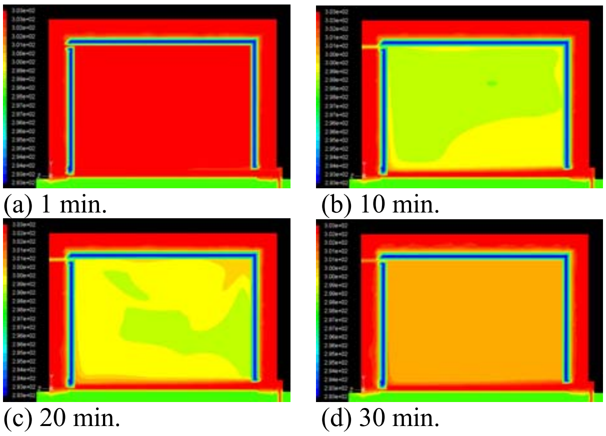

Fig. 5. (a)-(d) Simulated indoor air temperature vs. time

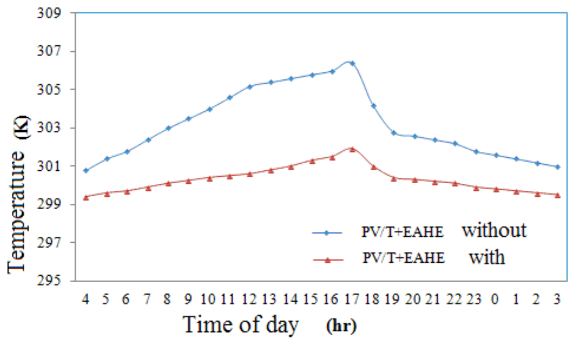

Fig. 8 Hourly variations of temperature of room air when operated with earth air heat exchanger (EAHE) for 24 h for a typical summer day.

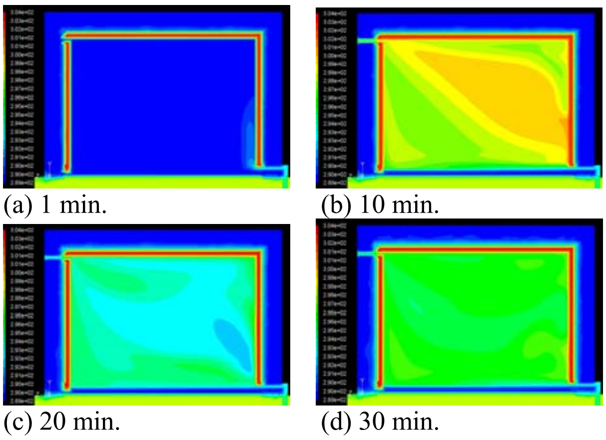

Fig. 6 (a)-(d) Simulated indoor air temperature vs. time

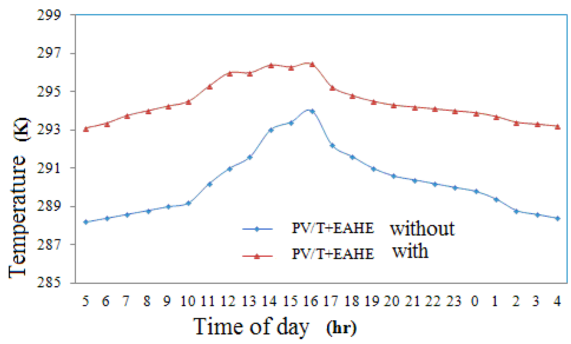

Fig. 9 Hourly variations of temperature of room air when operated with earth air heat exchanger (EAHE) for 24 h for a typical winter day.

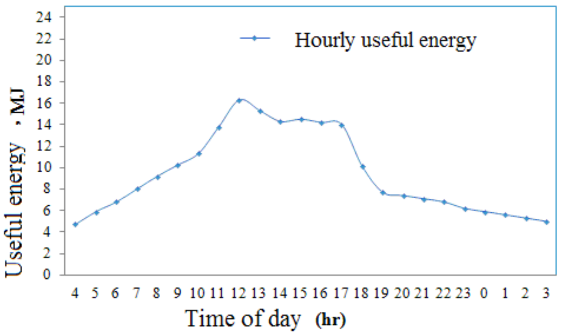

Fig. 10 Variation of hourly useful energy (MJ) when operated with photovoltaic (PV/T) and earth air heat exchanger (EAHE) for 24 hr for a typical summer day.

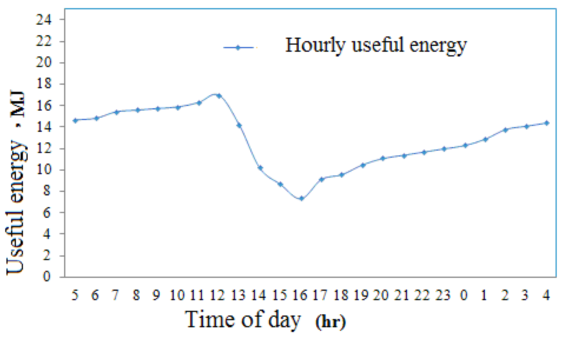

Fig. 11 Variation of hourly useful energy (MJ) when operated with photovoltaic (PV/T) and earth air heat exchanger (EAHE) for 24 hr for a typical winter day.

Table 1：Properties of the building materials

Materials	P (kgm^{-3})	C_p ($kJkg^{-1}°C^{-1}$)	K ($Wm^{-1}°C^{-1}$)	U ($Wm^{-2}°C^{-1}$)
SSPCM	850	1.0	0.2	-
Concrete	2500	0.92	1.75	-
Wood	500	2.5	0.14	0.875
Ground	2600	2.2	0.52	-

Table 2：Weather data of Hsin-Chu City

Season	Temperature (℃)	Wind speed (ms^{-1})	Pressure (Pa)
Summer	29.6	6 (Southern wind)	1044.8
Winter	15.9	6.6 (Northern wind)	1017

Table 3： Convergence criteria

continuity	x-velocity	y-velocity	z-velocity	energy
0.001	0.001	0.001	0.001	1e-06

Table 4: Average indoor air temperature vs. time for SSPCM+EAHE storage energy, absorption heat

Time min	concrete	indoor-air	floor-wood	EAHE	airout
1	302.99	302.75	302.98	302.74	302.74
5	302.95	300.42	302.92	302.74	300.53
10	302.91	299.38	302.84	302.74	299.38
20	302.83	299.56	302.68	302.74	299.68
30	302.76	300.52	302.53	302.74	300.63
60	302.55	300.87	302.14	302.74	300.97

Table 5: Average indoor air temperature vs. time for SSPCM+EAHE release energy, removal heat

Time min	concrete	inside-air	floor-wood	EAHE	airout
1	289.01	289.42	289.02	291.33	289.35
5	289.06	291.90	289.13	291.35	291.78
10	289.12	298.31	289.27	291.35	298.36
20	289.23	293.78	289.54	291.36	294.04
30	289.28	294.42	289.67	291.36	294.37
60	289.34	295.93	289.79	291.36	295.74

綠色建築三合一整合光伏電熱太陽能板(PV/T)空氣收集器,地熱空氣交換器(EAHE)及鋪設穩態形狀相變材料地板(SSPCM)的能量與最大可用能之分析研究

蔡博章[1]、張宇志[2]、賴世傑[3]
[1]中華大學機械工程研究所教授
[2,3]中華大學機械工程研究所研究生
國科會計畫編號.: NSC 99-2221-E-216-030

摘要

建築物越來越注重本身自己就是節能減碳有效率，因此自然通風、太陽能加溫與致冷、地溫空氣熱交換、自然光線及避陽遮蔭…等自然被動式不需要消耗太多能量的設置，將是綠色建築的不二選擇，本研究三機一體將薄膜光伏電熱太陽能板空氣收集器(PV/T aircollector), 收集熱氣驅動氣流、搭配地溫空氣熱交換(EAHE)來的氣流與吸收透過窗戶或太陽能板光線的穩態形狀相變材料地板(SSPCM)之儲熱儲能，利用新設計分階相變活塞氣缸壓氣機作系統氣流、溫度的自然調配，整合出一棟完全被動式混成系統建築。考慮新材料與建築服務結合的綠色設計新觀念，再以一棟位於台灣新竹地區沒有空調的建物為探討對象，來數值分析仲夏夜晚通風情況下，氣、電及熱的需求與影響，分析時程含蓋日、月及年，先針對薄膜光伏電熱太陽能板與各次系統之物理數學模型(Model)驗證，再發展出被動式混成系統建築的完整物理數學模型，搭配MATHLAB、CFD 軟體協助而得到分析解及數值解。致於現在正在進行利用熵值公式(enthalpy formulation)及Voller 與Patankar 之控制容積數值技

術求解二維暫態能量守恆搭配Stefan 移動邊界問題之福傳程式組Hybrid-HVAC，也將配合本棟被動式混成系統建築的個別次系統做程式修改為Hybrid-HVACP，此程式可以幫忙材料作驗證，以及協助太陽能電池空氣收集器、地溫空氣熱交換及穩態形狀相變材料地板等系統作設計，為綠色建築-節能省能屋的最佳化設計與能量分析，提供有利的工具。本研究將花費一年時間發展，以2010 年8 月1 日到31日0am-24pm 及2011 年各個月新竹市的氣象資料當樣本，設定系統與次系統參數到本樣品屋，進行可行性評估、加溫與致冷能力分析、空調性能、次系統操作條件改變時如空氣流量改變，環境溫度與室內溫度的變化及隨氣候分級環境溫度變化時，本被動式混成系統建築的逐月逐年的能量分析…等，希望本研究成果能協助居民對各式各樣節能省能技術作選擇，並促成人們有健康、舒適地居住環境的美夢能成真。

關鍵字:光伏電熱太陽能板空氣收集器、地溫空氣熱交換、穩態形狀相變材料、空調系統、太陽能。

三、參考文獻

本研究所引用之文獻參考已載明於二、報告內容之第七項文獻參考。另本研究成果及參與人員之衍生成果著作於文獻的有:

國際期刊論文有3篇: (Accepted)

1. Bor-Jang Tsai 、Koo-David Huang and Chien-Ho Lee , “Hybrid Structural Systems of An Active Building Envelope System(ABE)”, *Advanced material research*, Vol. 168-170. pp. 2359-2370. NSC-98-2221-E-216-047 (EI: ISTP)
2. Bor-Jang Tsai ,Yu-Jhih Jhang and Teh-Chau Liau, “Theoretical performance of integrated photovoltaic /thermal air collector, earth-air heat exchanger and greenhouse with a floor of shape-stabilized phase-change material: evaluation by energetic analyses”, *Advanced Science Letters* , in press. NSC-99-2212-E-216-030 (SCI: EI: IF: 1.35)
3. Bor-Jang Tsai, Sheam-Chyun Lin and Wei-Kuo Han, “Thermal analysis of a high power LED multi-chip package module”, *International Journal of Energy*, Issue 4, Vol. 5, pp. 79-87, 2011 NSC-99-2212-E-216-030 (EI)

國際期刊論文有1篇: (Reviewing)

4. Bor-Jang Tsai、Sheam-Chyun Lin and Wei-Cheng Yang, “HVAC analysis of a building installed shape stabilized phase change material plates coupling an active building envelope system”, *WSEAS Transactions Journal,* paper no. 53-895. (SCI: EI: IF:0.9)

國外研討會論文有5篇:

1. Bor-Jang Tsai , Koo-David Huang and Chien-Ho Lee,” Hybrid Structural Systems of An Active Building Envelope System(ABE)”, 2011 International Conference on Structures and Building Materials-Advanced Materials Research, 廣州, 中國, Jan. 2011.
2. Bor-Jang Tsai、Sheam-Chyun Lin and Wei-Cheng Yang, “Numerical HVAC Analysis of Shape-Stabilized Phase Change Material Plates Coupling an Active Building Envelope System in a Building”, WSEAS/NAUN International Conferences: 2nd International Conference on Fluid Mechanics and Heat and Mass Transfer 2011 (FLUIDSHEAT'11), Corfu Island, Greece., July 2011.
3. Bor-Jang Tsai, Sheam-Chyun Lin and Wei-Kuo Han,” Thermal Analysis of a high power LED multi-chip Package Module for Electronic Appliances”, WSEAS/NAUN International Conferences: 2nd International Conference on Fluid Mechanics and Heat and Mass Transfer 2011 (FLUIDSHEAT'11), Corfu Island, Greece., July 2011.
4. Sheam-Chyun Lin, Bor-Jang Tsai and Cheng-Ju Chang, “Influence of Elevator Moving Pattern and Velocity on the Airflow Uniformity for an LCD Panel Delivery Facility”, WSEAS/NAUN International Conferences: 2nd International Conference on Fluid Mechanics and Heat and Mass Transfer 2011 (FLUIDSHEAT'11), Corfu Island, Greece., July 2011.
5. Bor-Jang Tsai ,Yu-Jhih Jhang, “Theoretical performance of integrated photovoltaic /thermal air collector, earth-air heat exchanger and greenhouse with a floor of shape-stabilized phase-change material: evaluation by energetic analyses” ICETI 2011, 墾丁屏東台灣, Nov. 11-15, 2011

國內研討會有1篇、碩士論文有一:

1. 楊位盛-數值分析建築物整合鋪設穩態形狀相變材料板(SSPCM)及主動式外表帷幕系統(ABE)之空調效應,中華大學機械工程研究所碩士論文，臺灣新竹市 Jan. 2011.

1. Bor-Jang Tsai(蔡博章)，Pang-Wei Wu(張宇志), “綠色建築三合一整合光伏電熱太陽能板(PV/T)空氣收集器, 地熱空氣交換器(EAHE)及鋪設穩態形狀相變材料地板(SSPCM)的能量與最大可用能之分析研究”，中國機械工程學會第二十八屆全國學術研討會論文集，中華民國一百年十二月十日、十一日，中興大學 台中市。

四、計畫成果自評

本研究承蒙國科會經費贊助，非常感謝，也在參與人員努力下，有不錯成果。

研究內容預期達成目標情況為:

預期完成工作項目

(1)Develop physical/ mathematic models for the passive hybrid system (OK)

(2)MATLAB 7.0 program develop to gain the analytical

solutions of the passive hybrid system (OK)
(3)Finite difference-Fortran program code Hybrid-HVACP programming (OK)
(4)Energy & Exergy analysis methods (OK)
(5)Heating/cooling, η ,COP, ACH and HVAC performance of the hybrid system (OK)

本研究之主要成果:

(1) The hybrid system's BIPV、TE、SSPCM heat sink and EAHE efficiency gains can ensure energy-efficiency and cleanness. They can also reduce the CO_2 emissions.
(2) The hybrid system has the low total input power and its use constitutes an active approach to energy-saving.
(3) SSPCM consists of paraffin as dispersed PCM and high-density polyethylene (HDPE) or another material as a supporting material. The total stored energy is comparable with that of traditional PCMs.
(4) SSPCMs of the ceiling and floor can use the same material, temperature range of 297 K to 300 K start energy stored cycle and temperature range of 289 K to 293 K start energy released cycle.
(5) Reducing the temperature difference between the ceiling and the floor to less than 4 K increases the comfortableness of humans.
(6) 297 K is the most comfortable temperature in the HsinChu area.
(7) The simulation results reveal that if the difference between the ground temperature and the ambient temperature is less than 5 K, such as in HsinChu city obtained results are unsatisfactory, so the use of EAHE in areas with a large temperature difference yields better results.
(8) The effect of EAHE is not superimposed on additive with the effect of SSPCM, many parameters need to be considered such as materials, size and operating characteristics, therefore the design optimization is needed.
(9)Working fluid air of EAHE may be replaced with water or refrigerant which has a much larger temperature range than air.
(10) Hourly useful thermal energy (MJ) when operated with photovoltaic (PV/T) system and with earth air heat exchanger (EAHE) for a typical summer day. It has been observed that at 12 pm, useful thermal energy is calculated as 16 MJ with the operation of photovoltaic/thermal (PV/T) system, then the useful thermal energy decreases due to fall of temperature during evening. And useful thermal energy continuously fall down to 4 MJ while between 3 and 4 am.
(11) hourly useful thermal energy (MJ) when operated with photovoltaic (PV/T) system and with earth air heat exchanger (EAHE) for a typical winter day. It has been observed that at 12 pm, useful thermal energy is calculated as 16 MJ with the operation of photovoltaic/thermal (PV/T) system, while between 4 and 5 pm, the useful thermal energy decreases due to fall of temperature during evening. It then increases to 14.5 MJ with the operation earth air heat exchanger during night.

相關成果數據正準備投稿J. of Applied Thermal Engineering or J. of Building and Environments。

合計有研討會6篇，期刊4篇(1篇準備中)，畢業碩士研究生1位。

真實體建造及實驗數據的驗證尚未周全，所以在申請專利過程尚需資源、經費及努力，但太陽能,風力及地熱等再生能源分析設計、系統規畫、建物之節能省能技術及熱流分析技術等，應可技轉到建築或營造及節能省能科技，Green Housing等行業上，希望更多資源、經費相信ABE,SSPCM, EAHE系統會快應用到人類生活。

附件四

國科會補助專題研究計畫項下出席國際學術會議心得報告

日期：100 年 10 月 26 日

計畫編號	NSC－ 99－2221 － E － 216 －030		
計畫名稱	**綠色建築三合一整合光伏電熱太陽能板(PV/T)空氣收集器,地熱空氣交換器(EAHE)及鋪設穩態形狀相變材料地板(SSPCM)的能量與最大可用能之分析研究**		
出國人員姓名	蔡博章	服務機構及職稱	中華大學機械工程系教授
會議時間	100 年 7 月 14 至 100 年 7 月 17 日	會議地點	**Corfu Island, Greece.** 科芙島, 希臘
會議名稱	(中文)第二屆流力、熱傳及質傳國際研討會 2011 (FLUIDSHEAT'11) (英文) The 2nd International Conference on Fluid Mechanics and Heat and Mass Transfer 2011 (FLUIDSHEAT'11)		
發表論文題目	(中文) 1. 數值分析建築物整合鋪設穩態形狀相變材料板(SSPCM)及主動式外表帷幕系統(ABE)之空調效應 2. 電子產品之高功率 LED 多晶片模組之熱分析 (英文) **1.** Numerical HVAC Analysis of Shape-Stabilized Phase Change Material Plates Coupling an Active Building Envelope System in a Building 2. Thermal Analysis of a high power LED multi-chip Package Module for Electronic Appliances		

一、參加會議經過: **適逢旅遊旺季及預算不足，無法訂到機票而取消口頭報告**

二、與會心得 **有註冊沒有出國沒有到希臘**

三、考察參觀活動(無是項活動者略)

四、建議

1. 希望在台灣舉辦類似之國際聯合研討會—有關於綠色能源科技

2. 希望增加出席國際學術會議之經費

五、攜回資料名稱及內容

1. Proceedings of the WSEAS/NAUN International Conferences 論文集及CD片(託人帶回)

六、其他

本次 the WSEAS/NAUN International Conferences 之重要內容及發表之論文

WSEAS/NAUN International Conferences

Corfu Island, Greece

July 14-17, 2011

[Proceedings of the 15th WSEAS International Conference on Systems (Part of the 15th WSEAS CSCC Multiconference)]

[Proceedings of the 15th WSEAS International Conference on Computers (Part of the 15th WSEAS CSCC Multiconference)]

[Proceedings of the 15th WSEAS International Conference on Circuits (Part of the 15th WSEAS CSCC Multiconference) and the 5th International Conference on Circuits, Systems and Signals (CSS '11)]

[Proceedings of the 15th WSEAS International Conference on Communications (Part of the 15th WSEAS CSCC Multiconference) and the 5th International Conference on Communications and Information Technology (CIT '11)]

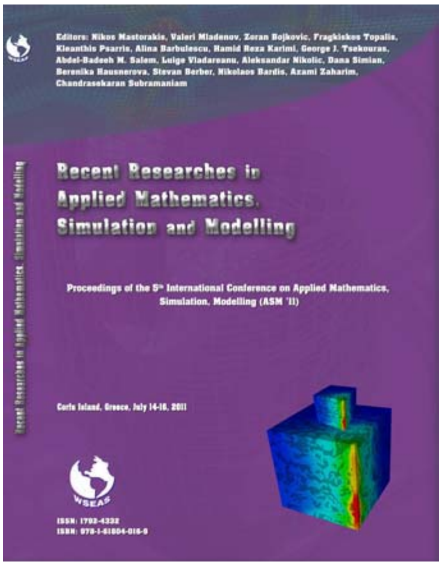

Proceedings of the 5th International Conference on Applied Mathematics, Simulation, Modelling (ASM '11)

Proceedings of the 8th WSEAS International Conference on Engineering Education (EDUCATION '11) and the 2nd International Conference on Education and Educational Technologies 2011 (WORLD-EDU '11)

Proceedings of the 4th WSEAS International Conference on Engineering Mechanics, Structures, Engineering Geology (EMESEG '11), the 2nd International Conference on Geography and Geology 2011 (WORLD-GEO '11) and the 5th International Conference on Energy and Development - Environment - Biomedicine 2011 (EDEB '11)

Proceedings of the 2nd International Conference on Fluid Mechanics and Heat and Mass Transfer 2011 (FLUIDSHEAT '11), the 2nd International Conference on Theoretical and Applied Mechanics 2011 (TAM '11), the 4th WSEAS International Conference on Urban Planning And Transportation (UPT '11) and the 4th WSEAS International Conference on Cultural Heritage and Tourism (CUHT '11)

WSEAS and NAUN Conferences

Joint Program

15th CSCC Multiconference:

15th WSEAS International Conference on Circuits

15th WSEAS International Conference on Systems

15th WSEAS International Conference on Communications

15th WSEAS International Conference on Computers

4th WSEAS International Conference on Urban Planning and Transportation (UPT '11)

4th WSEAS International Conference on Cultural Heritage and Tourism (CUHT '11)

8th WSEAS International Conference on Engineering Education (EDUCATION '11)

4th WSEAS International Conference on Engineering Mechanics, Structures, Engineering Geology (EMESEG '11)

International Conference on Applied Mathematics, Simulation, Modelling (ASM '11)

International Conference on Circuits, Systems and Signals (CSS '11)

International Conference on Communications and Information Technology (CIT '11)

International Conference on Fluid Mechanics and Heat and Mass Transfer 2011 (FLUIDSHEAT '11)

International Conference on Theoretical and Applied Mechanics 2011 (TAM '11)

International Conference on Education and Educational Technologies 2011 (EDU '11)

International Conference on Geography and Geology 2011 (GEO '11)

International Conference on Energy and Development - Environment - Biomedicine 2011 (EDEB '11)

Corfu Island, Greece, July 14-17, 2011

1st Day, July 14, 2011

Registration: 08:00-09:00

Keynote Lecture 1: 09:00-09:45, Room A'

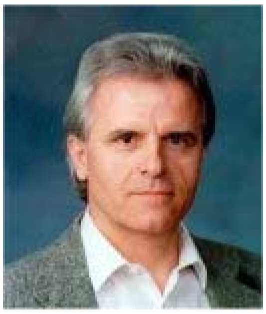

Fundamental Laws of Nature: Mass-Energy, Work, Heat and Entropy - From Reversible Isentropic to Irreversible Caloric Processes
by Prof. M. Kostic, Northern Illinois University, USA.

Keynote Lecture 2: 09:45-10:30, Room A'

Jet Noise Predictions Using Large Eddy Simulations

by Prof. Anastasios Lyrintzis, Purdue University, USA.

Keynote Lecture 3: 10:30-11:15, Room A’

Fuel Cell for Electric Locomotive Transportation:

State-of-the-Art Review and Challenges

by Prof. Pradip Majumdar, Northern Illinois University, USA.

Coffee-break: 11:15-11:45

Plenary Lecture 1: 11:45-12:30, Room A’

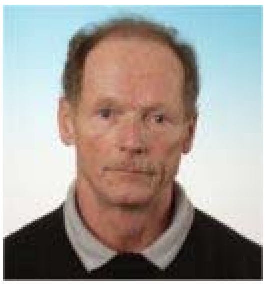

New Approach to Continuous and Discrete-Time Systems based on Abstract State Space Energy

by Prof. Milan Stork, University of West Bohemia, CZECH REPUBLIC.

Plenary Lecture 2: 11:45-12:30, Room B’

Romania, Tourism and Culture Major Drivers of Regional Attractiveness

by Prof. Mirela Mazilu, University of Craiova, ROMANIA.

Plenary Lecture 3: 11:45-12:30, Room C'

Intelligent Robotic System with Fuzzy Learning Controller and 3D Stereo Vision

by Prof. Shiuh-Jer Huang, National Taiwan University of Science and Technology, TAIWAN.

Plenary Lecture 4: 11:45-12:30, Room D'

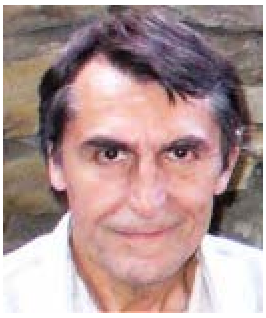

Infrared Image Processing Methods and Systems

by Prof. Alexander Bekiarski, Technical University Kliment Ohridski, BULGARIA.

CONFERENCE ROOM B’: 16:30-19:00

FLUIDSHEAT Session: Fluid Mechanics and Aerodynamics

Chair: Bor-Jang Tsai, Irina Eglite

Numerical HVAC Analysis of Shape-Stabilized Phase Change Material Plates Coupling an Active Building Envelope System in a Building	Bor-Jang Tsai, Sheam-Chyun Lin, Wei-Cheng Yang	303-250
Experimetal Study of Full Cone Spray Nozzle by Interferometry Particle Sizing Technique	D. Jasikova, M. Kotek, T. Lenc, V. Kopecky	303-240
Dynamics of Condensate Migration in Porous Media Under Ambient Treatments	Eko Siswanto, Hiroshi Katsurayama, Yasuo Katoh	303-171
Asymptotic Analysis of Stability of Slightly Curved Two-Phase Shallow Mixing Layers	I. Eglite	303-242
Experimental Evaluation of Backsplash on Falling Film Tube Bundles with Smooth Cooper Tubes	Libor Chroboczek, Jiri Pospisil, Zdenek Fortelny, Pavel Charvat	303-351
Scaled Experiment for Loss of Vacuum Accidents in Nuclear Fusion Devices: Experimental Methodology for Fluid-Dynamics Analysis in STARDUST Facility	M. Benedetti, P. Gaudio, I. Lupelli, A. Malizia, M. T. Porfiri, M. Richetta	303-276
A Channel Flow Affected by a Synthetic Jet Array – An Experimental Study	Petra Dancova, Zdenek Travnicek, Tomas Vit, Michal Kotek	303-297
Numerical Investigation on Performance and Environmental Impact of a Compound Wing in Ground Effect	S. Jamei, A. Maimun, S. Mansor, N. Azwadi, A. Priyanto	303-386

Numerical HVAC analysis of shape-stabilized phase change material plates coupling an active building envelope system in a building

Bor-Jang Tsai、Sheam-Chyun Lin and Wei-Cheng Yang

Abstract—Effect of shape-stabilized phase change material (SSPCM) plates combined with night ventilation in summer is investigated numerically. A building in Hsinchu, Taiwan without active air-conditioning is considered for analysis, which includes SSPCM plates as inner linings of walls、 the ceiling and floor, and an active building envelope system (ABE) is installed as well in the room becomes the Hybrid system. Unsteady simulation is performed using a verified enthalpy model, with time period covering the summer season. In the present study, a kind of floor with SSPCM is put forward which can absorb the solar radiation energy in the daytime or in summer and release the heat at night or in winter. In the present paper, the thermal performance of a room using such floor、wall and ceiling were numerically studied. Results show that the average indoor air temperature of a room with the SSPCM floor was about 2 K to 4 K higher than that of the room without SSPCM floor, and the indoor air temperature swing range was narrowed greatly. This manifests that applying SSPCM in room suitably can increase the thermal comfort degree and save space heating energy in winter.

Keywords— Shape-stabilized phase change material, Active building envelope system, HVAC, Renewable energy

Vortex

Professor Bor-Jang Tsai is with the Department of Mechanical Engineering Chung Hua University, HsinChu, Taiwan. (Phone: 886-3-5186478; Fax: 886-3-5186521; e-mail: bjtsai@chu.edu.tw)

Professor Sheam-Chyun Lin is with the Department of Mechanical Engineering National Taiwan University of Science and Technology Taipei, Taiwan. (Phone: 886-2-27333141#6453; fax: 886-2-27376460; e-mail: sclynn@mail.ntust.edu.tw)

Graduate student Wei-Cheng Yang is with the Department of Mechanical Engineering Chung Hua University, HsinChu, Taiwan. (Phone: 886-3-5186465; fax: 886-3-5186521; e-mail: chocolate0082 @hotmail.com)

I. Introduction

Energy storage not only reduces the mismatch between supply and demand but also improves the performance and reliability of energy systems and plays an important role in conserving the energy [1, 2]. It leads to saving of premium fuels and makes the system more cost effective by reducing the wastage of energy and capital cost. One of prospective techniques of storing thermal energy is the application of phase change materials (PCMs). Unfortunately, prior to the large-scale practical application of this technology, it is necessary to resolve numerous problems at the research and development stage. One of problems is so called the Stefan problem [3]. The heat transfer characteristics of melting and solidification process arise in the presence of phase change and expressing the energy conservation across the interface.

A. Shape-stabilized PCM (SSPCM)

In recent years, the Stefan problem has been resolved, a kind of novel compound PCM, the, Shape-stabilized PCM (SSPCM) has been attracting the interests of the researchers [4–6]. Fig. 1 shows the picture of this PCM plate. It consists of paraffin as dispersed PCM and high-density polyethylene (HDPE) or other materials as supporting material. Since the mass percentage of paraffin can be as much as 80% or so, the total stored energy is comparable with that of traditional PCMs.

Zhang et al. [7] investigated the influence of additives on thermal conductivity of SSPCM and analyzed the thermal performance of SSPCM floor for passive solar heating. To the authors' knowledge, no research work reported in the literature has made on the performance of shape-stabilized PCM application coupling the active building envelope system (ABE) in buildings combined with night ventilation. Therefore, the purpose of this study is to perform a numerical analysis on the thermal effect of shape-stabilized PCM plates as inner linings on the indoor air temperature under night ventilation conditions in summer, coupling the ABE system in a building, and for overall system of the building based upon a simulated room; a generic enclosure, combined with the climate report of Hsinchu city, Taiwan, 0am~24pm, 1^{st} ~6^{th} July., 2008. [8] to investigate: (1) feasibility study of the hybrid system (2) heating capability analysis (3) cooling capability analysis (4) indoor temperature levels. For the sake of simplification, thermal performance is the only consideration.

B. Active building envelopes

A brief description of the proposed ABE system is provided here (see Fig. 2). For more details, see [9]. The ABE system is comprised of two basic components: a photovoltaic unit (PV unit) and a thermoelectric heat pump unit (TE unit). The PV unit consists of photovoltaic cells, which are solid-state devices that convert solar radiation energy into electrical energy. The TE unit consists of thermoelectric heaters/coolers (referred to here onwards as TE coolers), which are solid-state devices that convert electrical energy into thermal energy, or the reverse. The PV and the TE units are integrated within the overall ABE enclosure. As shown in Fig. 2, the PV unit forms an envelope surrounding the external wall such that a gap is maintained between the wall and the PV unit. This gap acts as an external heat dissipation zone for the TE unit. The external walls of the proposed ABE system consist of two layers, as shown in Fig. 2.

The author's team; Tsai BJ [10] just finished a project; In a building installed the ABE system without SSPCM, wind、solar driven, bypass the windmill flow as a air flow, ambient temperature, To is equal to 308 K and indoor temperature, T_i is 301 K. Numerical results show the Ti will decrease 2 K when the ABE operating with heat sinks, without fan. As fan is opened, strong convective heat transfer, T_i will decrease approximately 4~5 K.

C. Hybrid system:

Zhou et al. [11] in 2009 reported effect of shape-stabilized phase change material (SSPCM) plates in a building (as shown Fig. 3) combined with night ventilation in summer is investigated numerically. Their conclusions show that the SSPCM plates could decrease the daily maximum temperature by up to 2 K due to the cool storage at night. Under the present conditions, the appropriate values for melting temperature, heat of fusion, thermal conductivity and thickness of SSPCM plates are 26 C, 160 kJ kg^{-1}, 0.5Wm^{-1} C^{-1} and 20 mm, respectively. The ACH at night needs to be as high as possible but the ACH at daytime should be controlled.

II. ANALYSIS METHOD—PHYSICAL AND MATHEMATIC ANALYSIS AND MODELING

The analysis is designed to examine the indoor thermal comfort level under night ventilation when the SSPCM plates are used or not. A typical south-facing middle room (room A shown in Fig. 3) in a multi-layer building in Hsinchu city, Taiwan, is considered as the model room for analysis, which has only one exterior wall (the south wall) and others are all interior envelopes. The dimension of the room is assumed as 3.9 m (length) x 3.3 m (width) x 2.7 m (height). The south wall is externally insulated with 60-mm-thick expanded polystyrene (EPS) board. There are a 2.1 m x 1.5 m double-glazed window and 1.5 m x 1.5 m ABE system in the south wall and a 0.9 m x 2 m wood door in the north wall which is adjacent to another room or the corridor. The overall heat transfer coefficients of the window and door are 3.01 and 0.875Wm^{-2} C^{-1}, respectively. SSPCM plates are attached to inner surfaces of four walls and the ceiling as linings. Based on a practical consideration, no SSPCM is included in the floor structure. Thermo-physical properties of SSPCM and materials of building envelopes are shown in Table 1. The summer climate data is generated by the software Medpha [8]. A verified enthalpy model [12] is applied for this simulation.

A. Heat transfer model of SSPCM wall and ceiling

The schematic of heat transfer through the exterior wall is shown in Fig. 4. The transient enthalpy equation is

$$\rho_j \frac{\partial H}{\partial t} = k_j \frac{\partial^2 T}{\partial x^2} \tag{1}$$

where for SSPCM, $H = \int_{T_0}^{T_1} c_{p,s} dT + \int_{T_1}^{T_2} c_{p,m} dT + \int_{T_2}^{T} c_{p,l} dT$

The initial condition is

$$T(x,t)_{t=0} = T_{init} \tag{2}$$

For the surfaces exposed to the outside and inside air, the boundary conditions are

$$q_{r,out} + h_{out}(T_{out} - T_{i,out}) = -k_i \left.\frac{\partial T}{\partial x}\right|_{x=0} \tag{3}$$

$$q_{r,in} + h_{in}(T_{in} - T_{i,in}) = -k_p \left.\frac{\partial T}{\partial x}\right|_{x=x_3} \tag{4}$$

For the exterior wall, $q_{r,in}$ and $q_{r,out}$ are indoor and outdoor radiation heat flux, respectively (Fig. 4). The convective coefficients h_{out} and h_{in} are calculated according to the ASHRAE Handbook [13].

The above equations are also applicable to interior walls and the ceiling. For the interior walls, h_{out} and $q_{r,out}$ are zero. For the ceiling (Fig. 5), the surface at $x=0$ is assumed insulated and the inner surface corresponds to convective heat transfer coefficient h_c and thermal radiation $q_{r,c}$. Thermal radiations among the internal surfaces of walls, floor and ceiling are calculated by thermal radiation network method [14].

B. Heat transfer model of the SSPCM floor

For floor construction shown in Fig. 6, the transient heat transfer equation is

$$\rho_j c_{p,j} \frac{\partial T}{\partial t} = k_j \frac{\partial^2 T}{\partial y^2} \tag{5}$$

Again, the initial condition is

$$T(y,t)_{t=0} = T_{init} \tag{6}$$

The boundary conditions are

$$\begin{cases} k_i \left.\dfrac{\partial T}{\partial y}\right|_{y=0} & y=0 \\ -q_{gap}+\varepsilon\sigma\left(T_{i,un}^4-T_{i,up}^4\right)=k_i\left.\dfrac{\partial T}{\partial y}\right|_{y=y_1} & y=y_1 \\ -q_{gap}+\varepsilon\sigma\left(T_{i,up}^4-T_{i,un}\right)=k_f\left.\dfrac{\partial T}{\partial y}\right|_{y=y_2} & y=y_2 \\ q_{f,up}+h_f\left(T_{in}-T_{f,up}\right)=k_f\left.\dfrac{\partial T}{\partial y}\right|_{y=y_3} & y=y_3 \end{cases} \quad (7)$$

Where $q_{f,up}$ is the radiation heat flux from the walls and ceiling to the wood floor.

C. Model of the indoor air of hybrid system building

The energy conservation equation fir the indoor air is

$$c_{p,a}\rho_a V_R \frac{dT_a}{dt} = \sum_{i=1}^{N} Q_{w,i} + Q_{s,c} + Q_L + Q_{win} + Q_{ABE} \quad (8)$$

Where $Q_{S,C}$ is assumed 70% of the total energy from the heat source [15], and $Q_{w,i}, Q_L$ and Q_{win} QABE [9,10] are calculated by the following equations:

$$Q_{win} = h_{in} \times \left(T_{w,i} - T_{in}\right) \times A_{w,i} \quad (9)$$

$$Q_L = c_{p,a}\rho_a V_R \times ACH \times \left(T_{out} - T_{in}\right)/3600 \quad (10)$$

$$Q_{win} = U_{win} \times \left(T_{out} - T_{in}\right) \times A_{w,i} \quad (11)$$

$$Q_{ABE} = Q_{ph} = Q_{pc} + IV \quad (12)$$

III. NUMERICAL TECHNIQUE

A. Description of the model room

The model room for analysis, which has dimension assumed as 3.9 m (length) x 3.3 m (width) x 2.7 m (height) concrete chamber. The thickness of chamber is 300mm, except the floor and the south wall each wall was installed 50mm thick SSPCM. The south wall is externally insulated with 60-mm-thick expanded polystyrene (EPS) board. There are a 2.1 m x 1.5 m double-glazed window and 1.5 m x 1.5 m ABE system in the south wall and a 0.9 m x 2 m wood door in the north wall which is adjacent to another room or the corridor. Floor is made of the first 30mm thick wood layer, under that the second layer is 40mm SSPCM layer, in between is the air layer with 30mm thick. And the extended computational domain is six times larger than that of the model room. (see Fig. 7)

B. Input parameters of the model room and applying software

In this study, using the Gambit to construct the solid model and grid mesh, then applying the Fluent as the solver of flow and thermal field. All parameters of the building and material properties of SSPCM were tabulated in Table 1. Regarding conditions of outside environments of the model room were listed in Table 2.

C. Establish grid cells

Cells of grid mesh of this model room as Fig. 8.

Outside environment (7505.784 m^3)：188520 cells
Concrete layer (11.565 m^3)： 285517 cells
SSPCM layer (2.364 m^3)：154989 cells
Inside air of room (18.72 m^3)：149760 cells
Floor-wood layer (0.2673 m^3)：7128 cells
Floor-air gap layer (0.2673 m^3)：7128 cells
Floor-SSPCM layer (0.3564 m^3)：7128 cells
Door-wood (0.09 m^3)：720 cells
Window-glass (0.21 m^3)：1680cells
Air layer front glass window (1.26 m^3)：4320 cells
Air layer front wood door (0.54 m^3)：10,080 cells

D. Initial conditions

The energy stored in cycle is: absorption heat

The ambient temperature is 303 K, 1atm and temperature of SSPCM layer is assuming a constant temperature 293 K, the optimal time (ie. Melting/fusing temperature, and its latent capacity is 265MJ/m^3。The initial condition (t=0) of indoor air temperature is assuming 303 K。 On the contrary,

The energy release in cycle is: removal heat

The ambient temperature is 289 K, 1atm and temperature of SSPCM layer is assuming a constant temperature 303 K, the optimal time (i.e. Melting/fusing temperature, and its latent capacity is 265MJ/m^3。The initial condition (t=0) of indoor air temperature is assuming 289 K。

Each time increment △t is 0.1 sec, then iterations up to the time we set, and need to satisfy the convergence criteria.

E. Boundary conditions

Using the embedding macro files of the Fluent to select our boundary conditions and our case is unsteady. And the maximum of solar radiation on the south wall is 900Wm^{-2} and the Hsin-Chu city in summer wind speed is southern 6 ms^{-1} 、average out door temperature is 302.96 K in winter wind speed is southern 6.6 ms^{-1} 、 average out door temperature is 288.9 K (see Table 2）。

F. Convergence criteria

For the purposes of solving any number of flow field changes in the iterative process, Simulation convergence criteria as shown in Table 3.

IV. RESULT AND DISCUSSION

A. Simulated temperature results of active ABE

Fig. 9 is the comparison of temperature distribution of active ABE for the fan was on (above) and off (below) in the summer. The gap is between solar panels and the TE wall as the hot side. The temperature can reach 313 to 318 K. Another side of TE produced the cooling effect, and through air-conditioning spread cool air to indoor space. Take the temperature condition at Y = 1.2m. The indoor temperature is 302 to 305 K with fan turning on, or the indoor temperature is about 304 to 307 without turning on the fan. The results show the fan can speed up TE cooling cold-side to spread quickly to the entire room.

B. Simulated temperature results of passive SSPCM

The energy stored in cycle is: absorption heat

The ambient temperature is 303 K, 1atm and temperature of SSPCM layer is assuming a constant temperature 293 K, the optimal temperature (ie. melting/fusing temperature, and its latent capacity is 265MJ/m^3。The initial condition (t=0) of indoor air temperature is assuming 303 K。Fig. 10 (a~d) simulated indoor air temperature vs. time (YZ plane at middle X) for the SSPCM in an energy stored cycle. At this time, initially t = 0, indoor air temperature is bigger than temperature of SSPCM layer, then all SSPCM layers start to absorb heat, Numerical results show as time increasing and the average indoor temperature will decrease. The average indoor temperature from 303 K drops to 295.93 K within 60 minutes. It produces cooling effect in the daytime or say in the summer. Except the average indoor temperature includes temperatures of wall-concrete、floor-wood、floor-air、door-wood and window-glass were tabulated in Table 4. On the contrary,

The energy release in cycle is: removal heat

The ambient temperature is 289 K, 1atm and temperature of SSPCM layer is assuming a constant temperature 303 K, the optimal time (i.e. Melting/fusing temperature, and its latent capacity is 265MJ/m^3。The initial condition (t=0) of indoor air temperature is assuming 289 K。Fig. 11 (e~h) simulated indoor air temperature vs. time (YZ plane at middle X) for the SSPCM in an energy released cycle. At this time, initially t = 0, indoor air temperature is smaller than temperature of SSPCM layer, then all SSPCM layers start to release heat, Numerical results show as time increasing and the average indoor temperature will increase. The average indoor temperature from 289 K climbs to 298.8 K within 60 minutes. It produces heating effect at night time or say in the winter. Except the average indoor temperature includes temperatures of wall-concrete、floor-wood、floor-air、door-wood and window-glass were tabulated in Table 5.

C. Comparison between numerical and analytical results for hourly variation of outdoor air temperature

Both of above discussions of SSPCM are idealized cases since the temperature of SSPCM was forced as constant, therefore latent heat capacity will be melting or fusing in a short period of time, and the temperature difference of the average indoor temperature will be large around 8 K to 9 K. In fact the average indoor temperature will be sinusoidal cycle with relation to optimal SSPCM temperature. The temperature differences of the average indoor temperature of both energy stored cycle and energy released cycle will around 2 K to 4 K. The analytical results have been reported by Xiao [16]. Therefore we can compare our numerical results with each other based upon hourly variation of outdoor air temperature in Hsin-Chu city on one day of July. (in here, indoor air temperature is simplified equal to outdoor air temperature). From Fig. 12 shows results of numerical and analytical are pretty consistent with each other.

V. CONCLUSIONS

The above numerical results coincide with each other. The active ABE system; a building installed the ABE system wind, solar driven, bypass the windmill flow as a air flow, ambient temperature, is equal to 308 K and indoor air temperature, 301 K. Numerical results show the indoor air temperature will decrease 2 K when the ABE operating with heat sinks, without fan. As fan is opened, strong convective heat transfer indoor air temperature will decrease approximately 4 K to 5K. Similarly, the hybrid system integrates the passive SSPCM system. The temperature differences of the average indoor temperature of both energy stored cycle and energy released cycle will around 2 K to 4 K. Hence the hybrid system will increase the function of ventilation. In comparison to natural convection, COP increases significantly, and it is quiet、 clean、energy-saving and cost-saving. Therefore, this study established a closer to the actual physical situation in Hybrid system as a whole, including sub-systems in this new analysis. Several brief summary as:

(1) The Hybrid system's BIPV、TE、SSPCM heat sink efficiency gains can achieve energy-efficiency and clean. It can also reduce the CO_2 emissions.

(2) The Hybrid system can reduce the total input power and achieve proactive approach to achieve energy saving goals.

(3) SSPCM consists of paraffin as dispersed PCM and high-density polyethylene (HDPE) or other materials as supporting material. The total stored energy is comparable with that of traditional PCMs.

(4) SSPCM of ceiling and floor can use the same material, temperature range between 297 K to 300 K start energy stored cycle, and temperature range between 289 K to 293 K start energy released cycle.

(5) Reduce the temperature gradient between ceiling and floor to under 4 K will increase the comfortableness of humans.

(6) 297 K is the most comfortable temperature.

VI. ACKNOWLEDGEMENT

We hereby express our thanks to the National Science Council for the support of research project NSC98-2221-E-216-047.

REFERENCES

[1] H. P. Garg, S. C. Mullick and A. K. Bhargava, " Solar

thermal energy storage", D. Reidel Publishing Co., 1985.
[2] Project Report. "Energy conservation through thermal energy storage", An AICTE Project, 1997.
[3] J. Stefan Uber einge problem der theoric der warmeleitung, S. B. Wein, Acad. Mat. Natur. 98:173–484,1989.
[4] H. Inaba and P. Tu Evaluation of thermophysical characteristics on shape-stabilized paraffin as a solid/liquid phase-change material. Heat Mass Transfer;32(4)307-12 ,1997.
[5] H. Ye and X. S. Ge "Preparation of polyethylene–paraffin compound as a form-stable solid–liquid phase change material", Solar Energy Mater Solar Cells;64(1):37–44 , 2000.
[6] Y. P. Zhang, R. Yang, H. F. Di, K. P. Lin, X. Xu and P. H. Qin. "Preparation, thermal performance and application of shape-stabilized PCM in energy efficient buildings." ,Collection of technical papers—2nd International energy conversion engineering conference AIAA, vol. 1 p. 600–610, 2004.
[7] X. Xu, Y. P. Zhang, K. P. Lin, H. F. Di and R.Yang "Modeling and simulation on the thermal performance of shape-stabilized phase change material floor used in passive solar buildings.", Energy Build;37:1084–91, 2005.
[8]Central Weather Bereau, Taipei, Taiwan: http://www.cwb.gov.tw/, 2008.
[9] S. Van Dessel, A. Messac and R. Khire, "Active building envelopes: a preliminary analysis", in: Asia International Renewable Energy Conference, Beijing, China, 2004.
[10] B. J. Tsai and J. H. Lee, "Active Building Envelope System(ABE): Wind & Solar driven Ventilation 、Electricity 、Heat pump", Proceeding of the 25th National Conference on Mechanical Engineering, The Chinese Society of Mechanical Engineers, Da-Yeh Univ. 2008. (NSC 96-2221-E-216-015)
[11] G. B. Zhou, Y. P. Yang, X. Wang and S. X. Zhou, "Numerical analysis of effect of shape-stabilized phase change material plates in a building combined with night ventilation", Applied Energy, Vol. 86, pp.52-59, 2009.
[12] G. B. Zhou, Y. P. Yang, K. P. Lin and W. Xiao, "Thermal analysis of a direct gain room of shape-stabilized PCM plates", Renewable Energy, Vol. 33, pp.1228-36, 2008.
[13] ASHRAE. ASHRAE handbook – Fundamentals, Chapter 3: Heat transfer. Atlanta: ASHRAE; 2001.
[14] Oppenheim AK. Radiation analysis by network method. Trans; ASME195665:725–35.
[15] C. K. Wilkins, R. Kosonen and T Laine, "An analysis of office equipment load factors", ASHRAE J. , 33:38–44, 1991.
[16] W. Xiao, X. Wang and Y. Zhang" Analytical optimization of interior PCM for energy storage in a lightweight passive solar room", Applied Energy, 86:2013–2018, 2009.

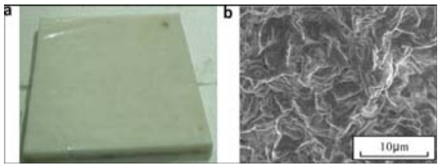

Fig. 1 The photos of the shape-stabilized PCM: (a) photo of the PCM plate; (b) electronic microscopic picture by scanning electric microscope (SEM) [6]

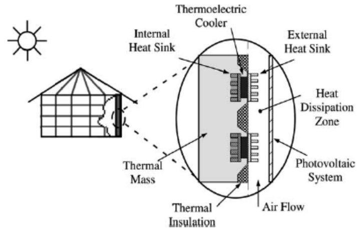

Fig. 2 Active building envelope (ABE) system [9]

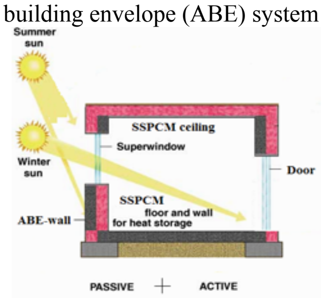

Fig. 3 Schematic of the simulated room with Hybrid system: profile of the room A with SSPCM and ABE wall

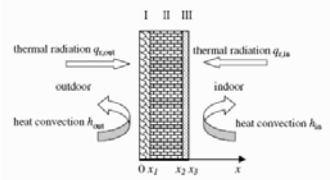

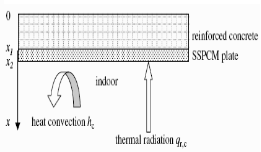

Fig. 4 Exterior wall surface

Fig. 5 Schematic of the ceiling heat transfer

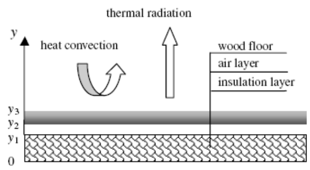

Fig. 6 The floor

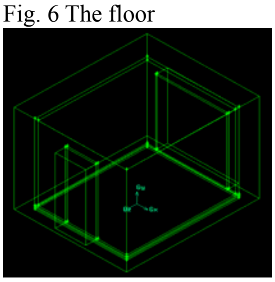

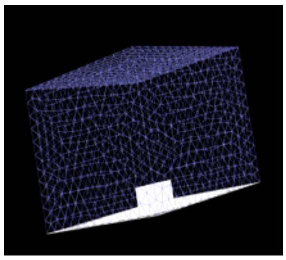

Fig. 7 Schematic diagram of the model room for analysis of a building。

Fig. 8 Grid mesh of the model room and environments

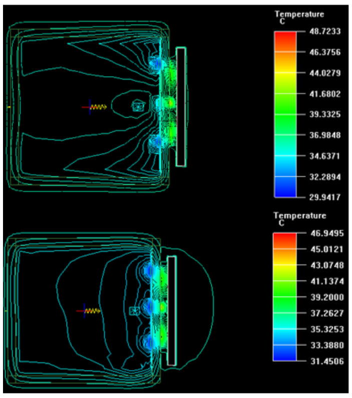

Fig. 9 Comparison of temperature distribution of the active ABE system for the fan was on (above) and off (below)

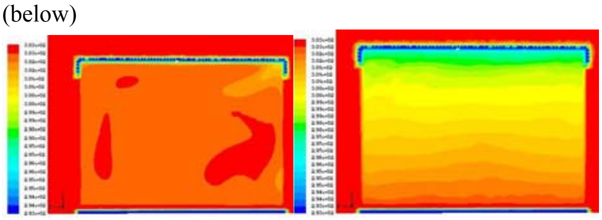

(a) 1 minutes (b) 5 minutes

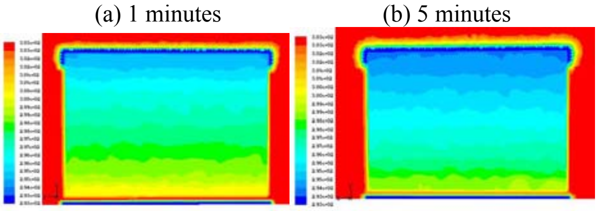

(c) 20 minutes (d) 60 minutes

Fig. 10 (a~d) Simulated indoor air temperature vs. time

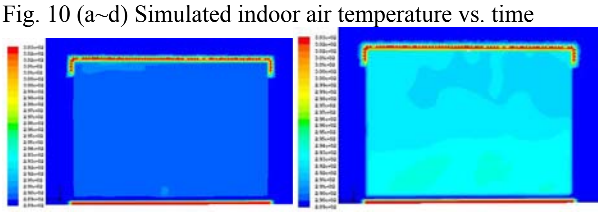

(e) 1 minutes (f) 5 minutes

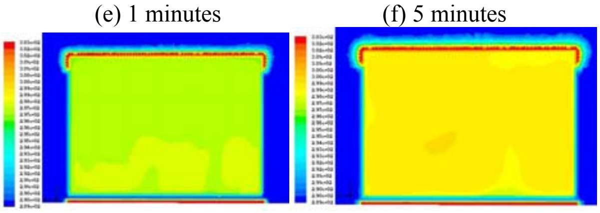

(g) 20 minutes (h) 60 minutes

Fig. 11 (e~h) Simulated indoor air temperature vs. time

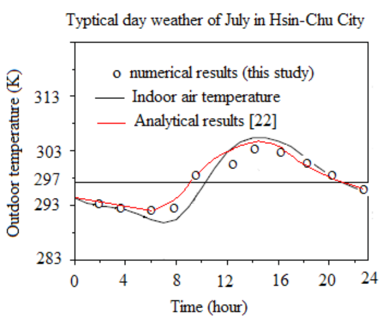

Fig. 12 hourly variation of outdoor air temperature in Hsin-Chu City。

Table 1：Material properties of the building

Materials	P (kgm^{-3})	C_p (kJkg^{-1}°C^{-1})	*K* (Wm^{-1}°C^{-1})	*U* (Wm^{-2}°C^{-1})
SSPCM	850	1.0	0.2	-
Concrete	2500	0.92	1.75	-
Win / Glass	1400	1.05	0.58	3.01
Door/Wood	500	2.5	0.14	0.875

Table 2：Weather data of Hsin-Chu City

Season	Temperature (℃)	Wind speed (ms^{-1})	Pressure (Pa)
Summer	29.6	6 (Southern wind)	1044.8
Winter	15.9	6.6 (Northern wind)	1017

Table 3： Convergence criteria

continuity	x-velocity	y-velocity	z-velocity	energy
0.001	0.001	0.001	0.001	1e-06

Table 4: Average indoor air temperature vs. time for SSPCM storage energy, absorption heat

Time min	concrete	indoor-air	floor-wood	floor-air	door-wood	Window glass
1	302.97	302.35	302.97	298.00	302.99	302.99
5	302.88	300.27	302.85	297.91	302.96	302.95
10	302.78	298.60	302.71	297.82	302.91	302.90
20	302.60	296.99	302.42	297.66	302.81	302.80
30	302.45	296.38	302.14	297.51	302.70	302.69
60	302.08	295.93	301.37	297.12	302.40	302.40

Table 5: Average indoor air temperature vs. time for SSPCM release energy, removal heat

Time min	concrete	inside-air	floor-wood	floor-air	door-wood	Window glass
1	289.03	289.83	289.03	296.00	289.00	289.01
5	289.16	292.78	289.19	296.06	289.05	289.06
10	289.30	295.09	289.40	296.17	289.12	289.13
20	289.55	297.28	289.83	296.41	289.26	289.28
30	289.76	298.12	289.27	296.63	289.40	289.43
60	290.29	298.80	291.47	297.25	289.82	289.84

Dr. Bor-Jang Tsai is currently Professor of Mechanical Engineering at Chung Hua University in HsinChu, Taiwan, Republic of China. Dr. Tsai earned his Ph.D from the School of Aerospace and Mechanical Engineering University of Missouri- Columbia in 1992, and had his M.S and B.S. in Mechanical Engineering from Clemson University, and Tatung University in 1984 and 1981, respectively. Professor Tsai's research interests cover: (1) Active building envelope system(ABE) ：Wind & solar driven ventilation、electricity、heat pump (2) Study of parameters affecting thermoelectric module performance (3) Hybrid structural systems of an active building envelope system(ABE) (4) Design and aerodynamic analysis of a flapping wing micro aerial vehicle (5) A Novel swiss-roll recuperator for the micro-turbine engine (6) Performance of a half-height innovative cooling Fan. Most of his researches are in areas of thermal fluid science, renewable energy, aerodynamic, gas turbine and green buildings.

Thermal Analysis of a high power LED multi-chip Package Module for Electronic Appliances

Bor-Jang Tsai, Sheam-Chyun Lin and Wei-Kuo Han

***Abstract*—**By using multiple high-power LEDs in products, some difficulties occur in predicting the temperature distribution because of the interaction of heat generated by each single-chip LED in the same module. To determine the heat dissipation of a multi-chip LED module, solid physical models for both single-chip and multi-chip LEDs with cooling fins were constructed. Simulation of the temperature distribution under natural convection was conducted using numerical analysis and by introducing formulas to estimate change in heat resistance. In addition to elucidating the heat dissipation of multi-chip LED modules, this study attempts to identify the major factors affecting the temperature distributions of LEDs.

Simulation results from the finite element program indicate that expressing the temperature distribution of a single LED chip using a spherical coordinate system is appropriate. The temperature curve of a copper plate away from the chip is nonlinear since the distribution curve declines dramatically and is no longer linear. The temperature of a multi-chip LED module is slightly less than that of linear superposition. A comparison of the estimated value for a multi-chip LED with the simulation result confirms the practicability and accuracy of the proposed thermal resistance formula in this work. This study provides reference data for estimating of thermal resistance in a multi-chip module.

***Keywords*—**LED(Light Emitting Diode), Heat dissipation, Thermal resistance

Vortex

Professor Bor-Jang Tsai is with the Department of Mechanical Engineering Chung Hua University, HsinChu, Taiwan. (Phone: 886-3-5186478; Fax: 886-3-5186521; e-mail: bjtsai@chu.edu.tw)

Professor Sheam-Chyun Lin is with the Department of Mechanical Engineering National Taiwan University of Science and Technology Taipei, Taiwan. (Phone: 886-2-27333141#6453; fax: 886-2-27376460; e-mail: sclynn@mail.ntust.edu.tw)

Graduate student Wei-Kuo Han is with the Department of Mechanical Engineering Chung Hua University, HsinChu, Taiwan. (Phone: 886-3-5186465; fax: 886-3-5186521; e-mail: chocolate0082 @hotmail.com)

I. INTRODUCTION

Most conventional Light Emitting Diode (LED) chips are small, approximately 0.16mm^2 in area and 0.11mm thick with 20mW input power and a low luminance level. Since 2000, the luminance efficiency of LEDs has increased and high-luminance LEDs have been developed. However, single-chip LEDs are insufficient as a light source. Thus, multi-chip modules are used currently. The advantages of an LED as a light source are single-color light emission, colorfulness, wide color range, no ultraviolet rays, small volume, light weight, and no environmental issues. However, an LED still has the disadvantage of inadequate luminance efficiency resulting in low LED light levels. Regular luminance requires hundreds to thousands of lumen. Conventional small chips fall far short of this luminance level. Currently, luminance is achieved using a large multi-chip array of LED chips. Conversely, use of a multi-chip high-power LED package is likely to produce a temperature exceeding 100^{o}C. Notably, thermal dissipation is difficult. Although an LED is a cold light source, luminance efficiency is currently low. These high temperatures decrease LED luminance efficiency and its capacity to emit light. Additionally, its lifespan is also greatly reduced. Therefore, the thermal resistance of an LED light module has a determining effect on product quality.

Using the definition and model of single-chip package thermal resistance in a multi-chip module remains difficult. Sofia [1] hypothesized that a heat source is available on a sectional thermal rod (conductor). Both ends of the thermal rod have fixed temperatures and the remaining parts are thermally insulated. The temperature distribution of a thermal rod is inversely linear distance from the heat source. Therefore, the principle of the heat transfer superposition model is established, which is represented by a thermal resistance matrix to account for insufficiencies of traditional thermal resistance analysis. This hypothesis cannot be applied to multi-chip LED modules because multi-chip LED thermal-dissipation base plates are generally not strip-shaped and contain heat sinks for convection. Nevertheless, interface temperatures measured for each chip coincide with theoretical basis of superposition in thermal conduction. Kim et al. [2] used instruments to measure the thermal resistance of multi-chips and substitute this thermal resistance into the superposition principle based upon the thermal resistance matrix. Thermal resistance system is then subdivided into LED chip thermal resistance and thermal resistance of the thermal dissipation base plate. When thermal resistance of the chip is significantly higher than the thermal resistance of the base plate dissipating into environment, the ratio of both is 10:1. As the number of chips increases, thermal resistance decreases. When the ratio of number of chips increases to thermal resistance is 1:1 or 1: 10, the number of chips has almost no effect on thermal resistance. The experiment in this study does not contain heat sink package modules. When tens to hundreds watts from a high-power LED chip package module are applied, the condition changes and such approach is infeasible. Thus, analysis of LED multi-chip applications for high-power LED multi-chip products is necessary. Thus, this study simulates a model with heat sink and discusses process in detail. Experiments will be performed next year.

Methods and analysis related to the application of the electrical method for junction temperature measurement applies thermal characterization of packaged semiconductor devices. This study is essential for anyone involved in the collection, interpretation, or application of semiconductor component thermal data, not only those in the LED industry but also those of developing new products such as high- frequency and high power devices with a total power dissipation of energy for a clock frequency of 200MHz and gate power switching requirement of 0.15 μW/NG/MHz [3]. Sikka, et al. identified the thermal and mechanical challenges of a multi-chip module (MCM) used in a high-end computer system. The chip and thermal paste carrier for an IBM MCM package [4]. A futuristic microprocessor package uses micro channels and an embedded thermoelectric device [5]. An innovative concept based on Advanced Thermal Solutions minimizes spreading resistance by using a Forced Thermal Spreader (FTS) in a BGA package [6] Along with optimizing spreading resistance, thermal transport must be managed to dissipate high heat fluxes in electronic devices. Such an example is provided by Colgan, et al. [7]. In their application, the chip operated at 400 W/cm^2. Micro channels were fabricated inside the package, for the required cooling during chip operation.

Therefore, analysis of multi-chip applications for high-power multi-chip products is necessary. In Year 2007, Sofia [8] used of thermal resistance measurements [9-11] and combined methods and analysis related to application of the electrical method for junction temperature measurement to thermally characterize packaged semiconductor devices, including using thermal transient data [12-15] to build the electrical thermal resistance measurements for hybrids and multi-chip packages. However, the illuminations of LEDs vary with junction temperature variation due to self-heating of LEDs and variation of ambient temperature. Hence, the thermal effect will affect both illumination intensity and output color of LED. Masana [16] derived a RC thermal model for a general semiconductor package. Muthu et al. [17] proposed a constant luminous model which ignores the thermal effect. Farkas et al. [18] developed a thermal model for luminous output and thermal I resistance in monochromatic light-emitting unit. Huang et al. [19, 20] derived a system dynamics model of a luminaire to relate the energy input to LED junction temperature.

II. OBJECTIVES OF ANALYSIS

First, this study focused on simulating the thermal resistance of an LED single-chip package, and the temperature distribution of an LED chip with a heat source on a copper plate. Error in thermal conduction of spherical coordinates was calculated. Then, the input power of this thermal resistance simulation of an LED single-chip package is divided into three levels, three various power inputs. Whether the temperature of an LED chip with the same position and structure as thermal resistance coincides with the superposition principle is discussed. Finally, four LED chips are arrayed at 2x2 pitches. Only one LED chip is illuminated to calculate thermal resistance based on the pitch between the copper plates. The four LED chips undergo linear temperature superposition, and then compared with four simulated LED chip temperatures when all are illuminated to verify the predicted accuracy of the four LED chips at 2x2 pitches.

A. Simulation of the CFdesign program

Single-chip LED illuminated with different power inputs.To verify CFdesign this program, a flat copper plate with four edge surfaces at 25^{o}C, top and bottom surfaces are insulated based upon Sofia's hypothesis (LED chip as point heat source without heat sink) was simulated and compared with the heat transfer calculation using spherical coordinates. This program is feasible for analyzing this LED multi-chip package module problem (Fig. 1). To verify whether the superposition principle model is suitable for LED chip cases, an LED single-chip is input with different powers to determine whether the temperature distribution is linearly proportion with respect to distance from top to bottom.

Multiple LEDs illuminated separately at a fixed LED pitch distribution.Although the package module has four LEDs, if the LEDs are arrayed symmetrically (Fig. 2), only one needs to be illuminated to determine temperatures of the other LEDs. The temperature difference between the LED chip interface and environment is utilized to calculate the temperature superposition and attain the final temperature of each chip when all four chips are illuminated simultaneously under the same power. The four chips illuminated simultaneously under the same power are simulated for verification.

Each LED chip in the package module is heated by current. According to thermal conduction theory, as the distance of an LED chip from a neighboring LED increases, the temperature drop increases. That is, the self-heating LED chip and the thermal effects of neighboring LED chips determine final temperature. Taking the four LED chips at 2x2 pitches as an example, the regular matrix distance is fixed at 8mm. This distance is the best choice discussions related to multi-chip temperature.

B. Establishment of the finite volume model and hypothesis

The CFdesign is adopted for finite element calculation of heat transfer. Temperature and heat flux of an LED chip module are also calculated.

Structure of and material in the chip module, notably, LED chips sized 1mmx1mm are typically studied. A blue sapphire 0.1mm thick in GaN chip structure is used to represent the current model (Fig. 2). The top surface of the structure 0mm in thick is the heat source surface

ISBN: 978-1-61804-020-6

setting that simplifies the heat source of the 5μm-thick epitaxial layer. Transparent silicone package material measuring 2 mm thick covers the LED chip to protect the chip and for light conduction. The base of the blue sapphire is attached to the copper plate. The copper plate is a commonly sold in markets. Size of it is simplified into a rectangle measuring 20mm long 20mm width, and 2mm thick. The copper plate dissipates heat. Heat is also conducted to the copper fin below it. Natural convection between the copper fin and atmosphere helps module thermal dissipation. Table lists the properties of materials.

Boundary conditions: Electrical power (1W) is considered when the model comes to input luminance. The Internal Quantum Efficiency (IQE) is 20%; the remainder, 0.8W, is released as heat. As luminance surface of the LED epitaxial layer down when the heat sink faces upward. The atmospheric temperature is set at 25 ^{o}C for natural convection. The computational domain of the LED light module is surrounded 7-times by the entire atmospheric layer as the simulation condition of natural convection.

C. *Equations for calculating thermal resistance between chips*

We assume the total thermal resistance of modules in a chip package is as follows:

$$R_{total}=R_{die}+R_{bonding}+R_{base}+R_{fin}+R_{fin-ambient} \qquad (1)$$

which, R_{die} ：LED chips thermal resistance,

$R_{bonding}$ ：Die layer thermal resistance,

R_{base} ：Copper plate thermal resistance,

R_{fin} ：Heat sink thermal resistance,

$R_{fin-ambient}$ ：Heat sink to atmospheric thermal resistance (thermal convection).

Although each LED chip does not heat up itself, neighboring LED chips will also be heated. However, the longer pitch distance, the less likely it is for neighboring LED chips to be affected. Thus, the chip pitch thermal resistance of LED multi-chip R_{pitch} is as shown in Fig. 3. Assuming LED chip area is small as compared to the entire package module, it may be regarded as a point heat source. Thermal conduction resembles a sphere that conducts heat outwards. The equation of pitch thermal resistance value for LED chip on copper plate surface may be estimated using spherical coordinates. It is inferred as follows:

Thermal conduction equation of spherical coordinates(r, Φ, and θ)

$$\frac{1}{r^2}\frac{\partial}{\partial r}\left(kr^2\frac{\partial T}{\partial r}\right)+\frac{1}{r^2\sin^2\theta}\frac{\partial}{\partial\phi}\left(k\frac{\partial T}{\partial\phi}\right)+\frac{1}{r^2\sin\theta}\frac{\partial}{\partial\theta}\left(k\sin\theta\frac{\partial T}{\partial\theta}\right)+\dot{q} = \rho c_p\frac{\partial T}{\partial t} \qquad (2)$$

Sphere radius r: internal radius is expressed as r_1 and external radius is expressed as r_2. Under a static condition, when the thermal conduction material is homogenous and isotropic and when the Azimuth angle Φ and polar angle θ are symmetrical structure. The simplified Eq. (1) is:

$$\frac{d}{dr}\left(r^2\frac{dT}{dr}\right)=0 \qquad (3)$$

The integral solution is,

$$T(r)=\frac{a}{r}+b \qquad (4)$$

Boundary conditions: heat flux is set as q_1" at $r=r_1$ and the heat source is the internal sphere surface. Temperature is set as T_2 at $r=r_2$ to define the temperature of the external sphere surface.

Fourier's Law:

When the heat source is at r_1

$$q_1''=-k\frac{dT}{dr}\Big|_{r}=r_1 \qquad (5)$$

$$a=r_1^2\frac{q_1''}{k} \qquad (6)$$

$$b=T_2-\frac{q_1''r_1^2}{k}\frac{1}{r_2} \qquad (7)$$

Substituting Eq. (5) ~ Eq. (7) into Eq. (3) to yields

$$T(r)=\frac{q_1''r_1^2}{k}\left(\frac{1}{r}-\frac{1}{r_2}\right)+T \qquad (8)$$

Thermal resistance is

$$R_{th}(r_1-r_2)=\frac{T_1-T_2}{q_1}=\frac{r_1^2}{A_1k}\left(\frac{1}{r_1}-\frac{1}{r_2}\right) \qquad (9)$$

III. RESULTS AND DISCUSSIONS

Based on simulation results, this study determines whether the temperature distribution is coincident with the linear superposition principle. Finally, four LED chips arrayed at a 2x2 *pitch* are used to ensure temperature prediction accuracy.

A. *Temperature depression curve is nonlinear*

After obtaining numerical simulation results of a single LED-chip, heat sink possesses geometric structural direction (Fig. 4). The direction of heat sink is expressed as vertical direction (V) while the other direction is expressed as parallel direction (P). Therefore, the contribution ratio of thermal conduction is higher compared with thermal convection (Figs. 5 and 6). However, the area of the LED from center to outer periphery is roughly 4mm, and has a symmetrical temperature distribution. This symmetrical temperature distribution is caused by the 2mm-thick copper plate and the 0.3mm-thick heat sink. They conducted heat symmetrically to the outside in a hemispherical manner.

After obtaining Eq. (8) results for thermal conduction of spherical coordinates (denote cal) and numerical simulation results of a single LED chip, the temperature decline is consistent with that of analytical calculation (Fig. 7). In other words, the heat sink has certain physical effects in thermal conduction. Nevertheless, since thermal convection is involved, the thermal dissipation mechanism is complex and requires further study.

B. *Linear superposition of copper plate temperature at the same position as below the LED*

After simulating results for three LED single-chip watt settings, the temperature of the copper plate below the LED (0.8mm) minus the environment temperature of 25°C serves as basis for reference. The 1/2-fold and 2-fold temperatures are added to the environment temperature to obtain results of copper plate temperature distributions of numerical simulation (by the superposition principle) and analytical calculation by the Eq. (8) for a LED single-chip package module under different powers (Fig. 8). Although these results may deviate by 2~7°C, estimation results still serve as reference. Among analysis, higher watts tend to result in overestimation of calculation values, because the temperature difference between fins of the heat sink and the atmosphere increases, heat dissipation increases, and the yielded temperature decreases to achieve thermal equilibrium.

C. *Thermal resistance comparison between a chip with and without attached soldering tin at same position of an LED chip*

Thermal resistance of a LED single-chip is simulated. The temperature differences between the LED (heat source) top surface and bottom surface, both attached soldering tin copper plate. They are consistent with calculated values by equations of formulas. Consequently, the thermal resistance yielded by equations of 1-D spherical coordinates is suitable for use for LED temperature predictions.

D. *Comparison of thermal resistance by numerical simulation and analytical estimation between an LED multi-chip*

In terms of thermal resistance of the entire LED chip module, the heat sink is subject to the greatest natural convection heat resistance *R(fin-a)*. The four LED chip symmetrical case shows that if one LED chip temperature can be measured, the thermal resistance equation can be used to calculate the temperature difference between the chip and copper plate (Fig. 2). The thermal resistance value from the first LED chip luminance surface to the second LED chip luminance surface is calculated as

$$R_{j1-j2} = R_{die1} + R_{bonding1} + R_{pitch}\left(= R_{th}\left(r_1 - r_2\right)\right) + R_{bonding2} + R_{die2} \quad (10)$$

When the heat source of LED chips is expressed as die1, based on result of one of the 0.8W chips, the heat flux of the contact surface between the LED and resin is only 0.0029W. This heat flux is negligible as it is too small. We hypothesize that all power is conducted from die1 to the copper plate and the thermal resistance of the pitched copper plate below of the first LED chip to the copper plate below the second LED chip; thus R_{pitch} is calculated by Eq. (9). When heat is conducted to die2, the thermal dissipation area of this LED is negligible as it is too small. The heat flux shows that the attached soldering tin heat flux below the non-heat source LED chip is negligible as it is too small. Therefore, the contribution of this thermal resistance can be neglected. Thus, Eq. (10) is expressed as

$$R_{j1-j2} \fallingdotseq R_{die1} + R_{bonding1} + R_{pitch} \quad (11)$$

Calculations for the symmetrical four LED chips at 2x2 pitch array are as follows :

$R_{j1-j2} = 3.492 + 1.222$

$R_{j1-j3} = 3.492 + 1.245$

$R_{j1-j4} = 3.492 + 1.222$

ΔT_{p2} = Temperature difference between horizontal chips

ΔT_{p3} = Temperature difference between adjacent chips

ΔT_{p4} = Temperature difference between vertical chips

$\Delta T_{p2} = \Delta T_{p4} = R_{j1-j2} \times Q = 3.77°C$

$\Delta T_{p3} = 3.79°C$

In this study, since the 8mm distance between two LED chips markedly exceeds cooper plate thickness and fin thickness (2.3mm), the temperature difference is overestimated and requires further study. In the same package, the interface temperature (T_{j1}) of input power of one LED chip is measured. Then, Eq. (11) calculates the four LED chips with the same simultaneous input power as results. The 4-fold watts greatly exceed the original 1-fold watts. Therefore, the junction interface temperature difference of 20°C at 111.9°C (numerical simulation) and 132.07°C (superposition calculation) is produced (Fig. 9). Although the single LED chip is overestimated, we infer to be attributed to the temperature difference between junction and heat sink. It is especially true for heat sink and atmospheric temperatures. The higher temperature difference between junction and heat sink is, the higher cooling efficiency will be. Therefore, the error in temperature calculated by superposition is related to heat generation of the high power. As the power increases, the likelihood of overestimating calculation will be. In the future, factors contributing to this error be examined to ensure accurate estimations

In view of the above results, it shows that the thermal resistance of different LED chip packages varies and that thermal dissipation devices (copper plates and heat sinks) have different mechanisms, therefore, thermal dissipation need to be calculated separately. The Eq. (10) is used to calculate the thermal resistance of the LED multi-chip to obtain the temperature of the LED multi-chip. Eq. (10) is expressed in matrix below:

$$(\left[R_{die}\right] + \left[R_{bonding}\right] + \left[R_{pitch}\right]) \times \left[Q\right] = \left[\Delta T_{junction-base}\right] \quad (12)$$

Thermal convection $R_{fin-ambient}$ will be incorporated in the calculation in the future to derive accurate estimations.

IV. CONCLUSIONS

Due to superposition of the LED multi-chip thermal distribution, calculation of heat dissipation becomes difficult. Arrangement of thermal management will likely increase difficult too. After systematic parameter analysis, we have increased knowledge of LED multi-chip package properties. Conclusions are summarized as follows.

(1) Simulation results for LED chip thermal dissipation indicate that the copper plate temperature depression curve distance away from the chip is non-linear.

(2) Under different powers, the temperature of the copper plate below the LED is feasible for superposition principle. Analytical estimation using addition is acceptable; however, as power inputs increases, calculated values will be overestimated. In this study, the interface temperature (T_{j1}) of input power of one LED chip is measured. Then, analytical calculates the four LED chips with the same simultaneous input power. The 4-fold watts greatly exceed the original 1-fold watts. Therefore, the junction interface temperature difference of 20°C at 111.9°C (numerical simulation) and 132.07°C (superposition calculation) is produced. The percentage of deviation is approximately 10%.

(2) Calculating the thermal resistance of 1-D spherical coordinates is suitable for use in predicting temperature differences in an LED structure.

(3) When the thickness of a copper plate is limited, LED multi-chip pitch thermal resistance of the copper plate can be calculated using equations of thermal resistance in 1-D spherical coordinates; however, the high wattage tends to result in overestimation of calculated values of thermal resistance.

(4) Comparison between the thermal resistance estimation and numerical simulation of LED multi-chip pitch shows that thermal resistance of an LED chip combined with a thermal dissipation copper plate should be calculated separately. The equation of thermal resistance is valuable as a reference.

V. ACKNOWLEDGEMENTS

The authors would like to thank ITRI for its support, and the National Science Council of the Republic of China, Taiwan, for financially supporting this research under Contract No. NSC98-2221-E-216-047

References

[1] J. W. Sofia, "Electrical thermal resistance measurements for hybrids and multi-chip packages", Analysis Tech, Wakefield, MA, USA, 1-9, 2000.

[2] Kim, Lan, *et al.*, "Thermal analysis of multi-chip LED packages", SPIE, 6355:P. 63550E. 2006.

[3] K. Azar, "Advanced cooling concepts and their challenges", Therminic conference, Innovation in Thermal Management, 1-38, 2002.

[4] K. Sikka, *et al.* "Multi-chip package thermal management of IBM z-Server systems", ITHERM, 2007. 7_Final_Program1.pdf

[5] R. Yavatkar, M. Tirumala, "Platform wide innovations to overcome thermal challenges", THERMES, 2007.

[6] "Forced thermal spreader characterization for an active_BGA", Internal memorandum, R&D Department, Advanced Thermal Solutions, Inc., 2006.

[7] E. Colgan, , *et al.*, "A practical implementation of silicon micro channel coolers for high power chips", SEMITHERM, 2005.

[8] J. W. Sofia, "Component thermal characterization: Transient to steady state, Analysis Tech", Wakefield, MA, USA, 1-36, 2007.

[9] Circuit-performance and thermal resistance measurements, (3100 Series) MIL-STD-750C, February, 1993

[10] A. D. Kraus, A. Bar-Cohen, "Thermal analysis and control of electronic equipment", McGraw Hill, Ch. 1, 1983.

[11] C. Neugebauer, *et al.* "Thermal response measurements for semiconductor devices", New York: Gordon & Breach Science Publications, Ch. 4, 5, 6, 1986.

[12] F. F. Oettinger, D. L. Blackburn, "Thermal resistance measurements", NIST Special Publication 400-86 from Series on Semiconductor Measurement Technology, July, 1990.

[13] M. Rencz, V. Szekely, *et al.*, "Determining partial resistances with transient measurements and using the method to detect die attach discontinuities", Eigtheenth Annual IEEE SEMI-THERM Symposium, 15-20, 2002.

[14] J. W. Sofia, "Analysis of thermal transient data with synthesized dynamic models for semiconductor devices", IEEE Transactions on Components, Packaging, and Manufacturing Technology Part A (CPMT), March, 18: 39-47, 1995.

[15] V. Szekely, M. Rencz, "Thermal dynamics and the time constant domain", IEEE Trans. on Comp. and Packaging Tech., 23(3) 687-694, 2000.

[16] F. N. Masana, "A new approach to the dynamic thermal modelling of semiconductor packages", Microelectron. Reliab. 41 (6) 901–912, 2001.

[17] S. Muthu, F.J. Schuurmans, M.D. Pashley, "Red green blue LED based white light generation": Issues and control, in: IAS'02, Proc. IEEE 1 (2002) 327–333.

[18] G. Farkas, Q.V. Vader, A. Poppe, G. Bognar, "Thermal investigation of high power optical devices by transient testing", IEEE Trans. Compon. Package. Technol. 28 (1) 45–50, 2005.

[19] B. J. Huang, P. C. Hsu, M. S. Wu, C. W. Tang, "Study of system dynamics model and control of a high-power LED lighting luminaire", Energy 32 (11) 2187–2198. 2007.

[20] B. J. Huang, C. W. Tang, M. S. Wu, "System dynamics model of high-power LED Luminaire", Applied Thermal Engineering 29 (4) 609–616, 2009

Figures

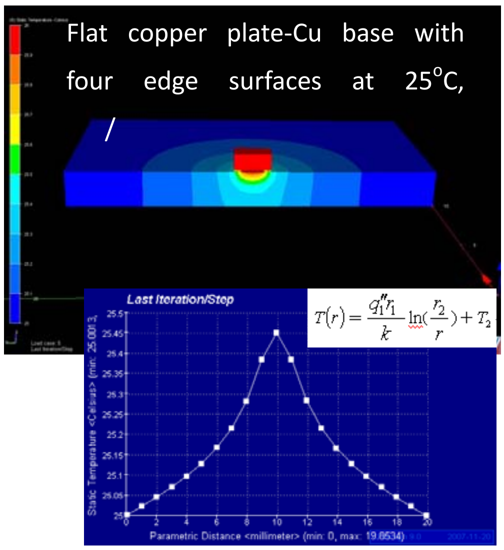

Fig. 1 Flat copper plate-Cu base (LED chip as a point heat source without a heat sink) the heat transfer calculation using spherical coordinates.

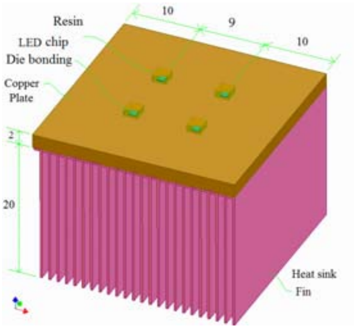

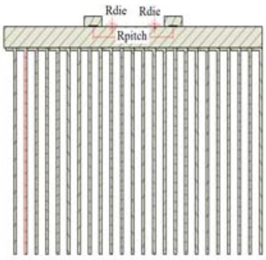

Fig. 2 Geometrical dimensions and materials of an LED 4-chip package module

Fig. 3 Schematic diagram of thermal resistance of an LED 4-chip package module

LED junction 64.7°C

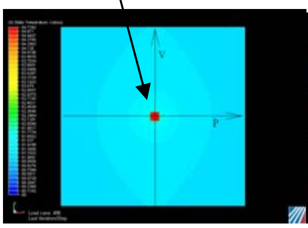

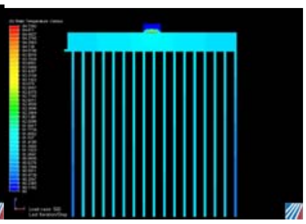

Fig. 4 Geometrical structure direction and temperature field of an LED single-chip package module (top view)

Fig. 5 Temperature field of an LED single-chip package module (front cross-sectional view)

$$T(r)=\frac{q_1'' r_1^2}{k}\left(\frac{1}{r}-\frac{1}{r_2}\right)+T_2$$

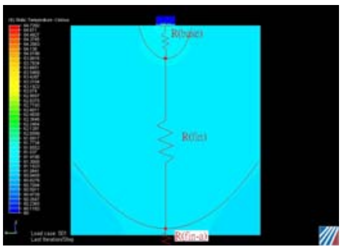

$$R_{th}(r_1-r_2)=\frac{T_1-T_2}{q_1}=\frac{r_1^2}{A_1 k}\left(\frac{1}{r_1}-\frac{1}{r_2}\right)$$

Fig. 6 Temperature field and analog circuit of thermal resistance for an LED single-chip package module (side view)

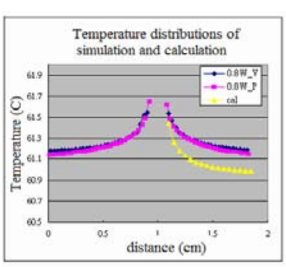

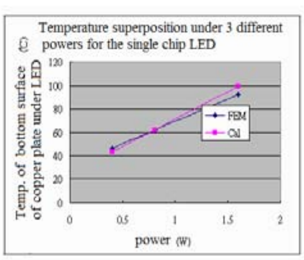

Fig. 7 Copper plate temperature depression curves by numerical simulation and analytical calculation by Eq. (8) for an LED single-chip package module

LED junction 97.4°C LED junction 46.9°C

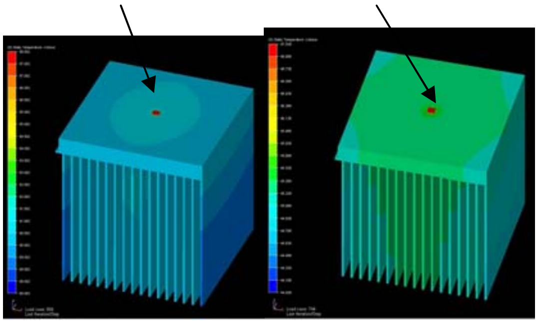

Single-chip LED 1.6W Single-chip LED 0.4W

Fig. 8 Copper plate temperature distributions by numerical simulation (via the superposition principle) and analytical calculation by Eq. (8) for an LED single-chip package module under varying power.

LED junction 54,6°C LED junction 112°C

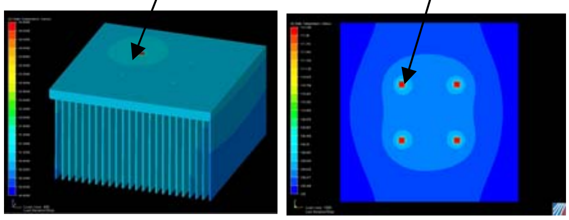

Fig. 9 Junction interface temperature distributions of a single-chip module and an LED 4-chip package module

Dr. Bor-Jang Tsai is currently Professor of Mechanical Engineering at Chung Hua University in HsinChu, Taiwan, Republic of China. Dr. Tsai earned his Ph.D from the School of Aerospace and Mechanical Engineering University of Missouri- Columbia in 1992, and had his M.S and B.S. in Mechanical Engineering from Clemson University, and Tatung University in 1984 and 1981, respectively. Professor Tsai's research interests cover: (1) Active building envelope system(ABE)：Wind & solar driven ventilation、electricity、heat pump (2) Thermal analysis of electronic appliances such as CPU and LED (3) Hybrid structural systems of an active building envelope system(ABE) (4) Design and aerodynamic analysis of a flapping wing micro aerial vehicle (5) A Novel swiss-roll recuperator for the micro-turbine engine (6) Performance of a half-height innovative cooling Fan. Most of his researches are in areas of thermal fluid science, renewable energy, aerodynamic, gas turbine and green buildings.

ISBN: 978-1-61804-020-6

Dear Dr.Alkis Polyrakis

Thank you very much for your assistance!

Bor-Jang Tsai

--- 11/10/26 (三)，WSEAS Support *<support@wseas.org>* 寫道：

寄件者: WSEAS Support <support@wseas.org>
主旨: NAUN / University Press Journals
收件者: stlouis17888@yahoo.com.tw
日期: 2011 年 10 月 26 日,三,下午 6:42

Dear Prof. / Dr.,

We would like to inform you that your paper was published in one of our journals. You may examine the attached file to track down the publication.

You are reminded that this journal will only be published electronically and no hard copies will be available.

Best Regards,

--
Alkis Polyrakis
WSEAS Editing Manager

Your paper was accepted. Registration deadline: July 1st

2011/5/20(五) 下午 9:13

寄件者:

"WSEAS Support" <support@wseas.org>

將寄件者加入至通訊錄

收件者:

stlouis17888@yahoo.com.tw

Message contains attachments

1 個檔案 (112KB)

Dear Prof. / Dr. [Name1],

This message is sent to all the authors of accepted papers.
We apologize if you receive multiple copies of this email.

We would like to inform you that your paper submitted to the International
conferences in Corfu Island, Greece, July 14-17, 2011 has been accepted for
publication in the conference proceedings. After the conference, CD-ROM and
Book proceedings will be sent to ISI, EI Compendex, SCOPUS, IET, Elsevier
and all the other indexes of http://www.wseas.us/indexes .
(Conferences are sponsored by IEEEAM, EUROPMENT, WSEAS)

The exact ID number and title of your accepted paper was sent to the author
who uploaded it via our web page. Please contact them if you have multiple
papers and you are not sure which of them we are referring to.

IMPORTANT: If you have more than one paper in this conference, please make
sure which of your papers are accepted before you register. If you are
unsure, contact us by e-mail.

Registration deadline: July 1st
Revised paper submission deadline: July 3rd

Note that the reviewers' comments will be sent to you after your

registration. You will also receive a username and password that will grant
you access to the WSEAS E-Library.

Please consult the attached form for your registration. You will need to
fill in the required information on the first page and send it to us either
by email or by fax.

E-mail: support@wseas.org (For papers with ID 655-xxx) -OR- E-mail:
books@europment.org (For papers with ID 510-xxx)
Fax: 0030 211 800 1964

Rayna Moskova
Alkis Polyrakis
WSEAS
Ag. I. Theologou 17-23
Zografou, 15773, Athens, Greece
Phone +30 210 747 3313
FAX +30 211 800 1964
URL: http://www.wseas.org

國科會補助計畫衍生研發成果推廣資料表

日期:2011/10/31

<table>
<tr><td rowspan="3">國科會補助計畫</td><td colspan="3">計畫名稱: 綠色建築三合一整合光伏電熱太陽能板(PV/T)空氣收集器,地熱空氣交換器(EAHE)及鋪設穩態形狀相變材料地板(SSPCM)的能量與最大可用能之分析研究</td></tr>
<tr><td colspan="3">計畫主持人: 蔡博章</td></tr>
<tr><td colspan="3">計畫編號: 99-2221-E-216-030-　　　　學門領域: 能源科技</td></tr>
<tr><td rowspan="2">研發成果名稱</td><td colspan="3">（中文）建築物系統整合技術：氣、電、熱及綠建材之整合規畫技術II</td></tr>
<tr><td colspan="3">（英文）</td></tr>
<tr><td>成果歸屬機構</td><td>中華大學</td><td>發明人
(創作人)</td><td>蔡博章,張宇志,賴世傑</td></tr>
<tr><td rowspan="2">技術說明</td><td colspan="3">（中文）建築物越來越注重本身自己就是節能減碳有效率，因此自然通風、太陽能加溫與致冷、地溫空氣熱交換、自然光線及避陽遮蔭…等自然被動式不需要消耗太多能量的設置，將是綠色建築的不二選擇，本研究三機一體將薄膜光伏電熱太陽能板空氣收集器(PV/T air collector), 收集熱氣驅動氣流、搭配地溫空氣熱交換(EAHE)來的氣流與吸收透過窗戶或太陽能板光線的穩態形狀相變材料(SSPCM)之儲熱儲能，整合出一棟完全被動式混成系統建築。考慮新材料與建築服務結合的綠色設計新觀念，再以一棟位於台灣新竹地區沒有空調的建物為探討對象，來數值分析仲夏夜晚通風情況下，氣、電及熱的需求與影響，分析時程含蓋日、月及年，先針對薄膜光伏電熱太陽能板與各次系統之物理數學模型(Model)驗證，再發展出被動式混成系統建築的完整物理數學模型，搭配MATHLAB、CFD 軟體協助而得到分析解及數值解。
利用熵值公式(enthalpy formulation)及Voller 與Patankar 之控制容積數值技術求解二維暫態能量守恆搭配Stefan 移動邊界問題幅與波數下，自然對流具有最佳的熱傳增益。之福傳程式組Hybrid-HVAC，也將配合本棟被動式混成系統建築的個別次系統做程式修改為Hybrid-HVACP，此程式可以幫忙材料作驗證，以及協助太陽能電池空氣收集器、地溫空氣熱交換及穩態形狀相變材料地板等系統作設計，為綠色建築-節能省能屋的最佳化設計與能量分析，提供有利的工具。</td></tr>
<tr><td colspan="3">（英文）Applying the thin film photovoltaic technology for building integration, and an integrated photovoltaic /thermal air collector, collect hot air driving air flow, mixing the air flow from earth air heat exchanger (EAHE) and hot air flow to the shape-stabilized phase change material (SSPCM) inside greenhouse, SSPCM also absorbs energy form solar lighting through windows and solar panels. A piston cylinder air compressor will adjust the moderate control of air flow and temperatures of ambient and room for the hybrid system. Theoretical performance assessment of this building is analyzed by using energy analysis methods based on Hsinchu weather. Mathematic model will be resolved by the helps of MATLAB 7.0 program. Energy needs of air-conditioning、electricity and thermal will be predicted. The Hybrid-HVACP and should be able to solve the hybrid system building with the PV/T、EAHE and SSPCM numerically in accuracy, then optimization design and energetic analysis of the building.</td></tr>
<tr><td>產業別</td><td colspan="3">建物裝修及裝潢業；熱能供應業</td></tr>
<tr><td>技術/產品應用範圍</td><td colspan="3">建築營造、房地產、節能省能及能源科技業。
建築物帷幕系統、建築物節能省能系統規畫
綠建築混成設計最佳化軟體</td></tr>
<tr><td>技術移轉可行性及預期效益</td><td colspan="3">綠建築
節能省能
能源材料
環保
氣電熱整合
Green Housing
Shape-stabilized Phase Change Materials
Save Energy and Protect Environment</td></tr>
</table>

註：本項研發成果若尚未申請專利，請勿揭露可申請專利之主要內容。

99 年度專題研究計畫研究成果彙整表

<table>
<tr><td colspan="3">計畫主持人：蔡博章</td><td colspan="5">計畫編號：99-2221-E-216-030-</td></tr>
<tr><td colspan="8">計畫名稱：綠色建築三合一整合光伏電熱太陽能板(PV/T)空氣收集器,地熱空氣交換器(EAHE)及鋪設穩態形狀相變材料地板(SSPCM)的能量與最大可用能之分析研究</td></tr>
<tr><td colspan="3" rowspan="2">成果項目</td><td colspan="3">量化</td><td rowspan="2">單位</td><td rowspan="2">備註（質化說明：如數個計畫共同成果、成果列為該期刊之封面故事...等）</td></tr>
<tr><td>實際已達成數（被接受或已發表）</td><td>預期總達成數(含實際已達成數)</td><td>本計畫實際貢獻百分比</td></tr>
<tr><td rowspan="15">國內</td><td rowspan="4">論文著作</td><td>期刊論文</td><td>0</td><td>0</td><td>100%</td><td rowspan="4">篇</td><td></td></tr>
<tr><td>研究報告/技術報告</td><td>1</td><td>0</td><td>100%</td><td>喜室(Hess Energy Co.)-有關綠建築之窗戶及門之綠色技術與節能省能的諮詢報告</td></tr>
<tr><td>研討會論文</td><td>1</td><td>1</td><td>100%</td><td>1.Bor-Jang Tsai(蔡博章)，Pang-Wei Wu(張宇志),
’ 綠色建築三合一整合光伏電熱太陽能板(PV/T)空氣收集器,地熱空氣交換器(EAHE)及鋪設穩態形狀相變材料地板(SSPCM)的能量與最大可用能之分析研究
’ ，中國機械工程學會第二十八屆全國學術研討會論文集，中華民國一百年十二月十日、十一日，中興大學 台中市。</td></tr>
<tr><td>專書</td><td>0</td><td>0</td><td>100%</td><td></td></tr>
<tr><td rowspan="2">專利</td><td>申請中件數</td><td>1</td><td>1</td><td>100%</td><td rowspan="2">件</td><td>專利名稱:主動式外表帷幕系統(ABE):風力太陽能驅動氣,電,熱之研究.撰寫申請書校內審查.</td></tr>
<tr><td>已獲得件數</td><td>0</td><td>0</td><td>100%</td><td></td></tr>
<tr><td rowspan="2">技術移轉</td><td>件數</td><td>1</td><td>1</td><td>100%</td><td>件</td><td>喜室(Hess Energy Co.)或台灣寶熊公司</td></tr>
<tr><td>權利金</td><td>1</td><td>1</td><td>100%</td><td>千元</td><td>技轉金 15000 元</td></tr>
<tr><td rowspan="4">參與計畫人力（本國籍）</td><td>碩士生</td><td>2</td><td>2</td><td>100%</td><td rowspan="4">人次</td><td>1.張宇志 2. 賴世傑</td></tr>
<tr><td>博士生</td><td>0</td><td>0</td><td>100%</td><td></td></tr>
<tr><td>博士後研究員</td><td>0</td><td>0</td><td>100%</td><td></td></tr>
<tr><td>專任助理</td><td>0</td><td>0</td><td>100%</td><td></td></tr>
<tr><td>國外</td><td>論文著作</td><td>期刊論文</td><td>4</td><td>2</td><td>100%</td><td>篇</td><td>三篇被接受及出版, 一篇審查中</td></tr>
</table>

							國際期刊論文有 3 篇:(Accepted) 1. Bor-Jang Tsai 、Koo-David Huang and Chien-Ho Lee,’Hybrid Structural Systems of An Active Building Envelope System(ABE) ’ , Advanced material research, Vol. 168-170. pp. 2359-2370. NSC-98-2221-E-216-047 (EI: ISTP) 2. Bor-Jang Tsai ,Yu-Jhih Jhang and Teh-Chau Liau, ’Theoretical performance of integrated photovoltaic /thermal air collector, earth-air heat exchanger and greenhouse with a floor of shape-stabilized phase-change material: evaluation by energetic analyses’, Advanced Science Letters , in press. NSC-99-2212-E-216-030 (SCI: EI: IF: 1.35) 3. Bor-Jang Tsai, Sheam-Chyun Lin and Wei-Kuo Han,’Thermal analysis of a high power LED multi-chip package module’, International Journal of Energy, Issue 4, Vol. 5, pp. 79-87, 2011 NSC-99-2212-E-216-030 (EI) 國際期刊論文有 1 篇:(Reviewing)

							4. Bor-Jang Tsai、Sheam-Chyun Lin and Wei-Cheng Yang, ' HVAC analysis of a building installed shape stabilized phase change material plates coupling an active building envelope system ', WSEAS Transactions Journal, paper no. 53-895. (SCI: EI: IF:0.9)
		研究報告/技術報告	0	0	100%		
		研討會論文	5	2	100%		國外研討會論文有5篇: 1.Bor-Jang Tsai , Koo-David Huang and Chien-Ho Lee, ' Hybrid Structural Systems of An Active Building Envelope System(ABE)', 2011 International Conference on Structures and Building Materials-Advanced Materials Research, 廣州, 中國, Jan. 2011. 2. Bor-Jang Tsai、Sheam-Chyun Lin and Wei-Cheng Yang, ' Numerical HVAC

							(FLUIDSHEAT'11), Corfu Island, Greece., July 2011. 3. Bor-Jang Tsai, Sheam-Chyun Lin and Wei-Kuo Han,' Thermal Analysis of a high power LED multi-chip Package Module for Electronic Appliances', WSEAS/NAUN International Conferences: 2nd International Conference on Fluid Mechanics and Heat and Mass Transfer 2011 (FLUIDSHEAT'11), Corfu Island, Greece., July 2011. 4. Sheam-Chyun Lin, Bor-Jang Tsai and Cheng-Ju Chang, ' Influence of Elevator Moving Pattern and Velocity on the Airflow Uniformity for an LCD Panel Delivery Facility', WSEAS/NAUN International Conferences: 2nd International Conference on Fluid Mechanics and Heat and Mass Transfer 2011 (FLUIDSHEAT'11), Corfu Island, Greece., July 2011. 5. Bor-Jang Tsai ,Yu-Jhih Jhang, ' Theoretical performance of integrated photovoltaic /thermal air collector, earth-air heat

							exchanger and greenhouse with a floor of shape-stabilized phase-change material: evaluation by energetic analyses ' ICETI 2011, 墾丁屏東台灣, Nov. 11-15, 2011
		專書	0	0	100%	章/本	
	專利	申請中件數	0	0	100%	件	
		已獲得件數	0	0	100%		
	技術移轉	件數	0	0	100%	件	
		權利金	0	0	100%	千元	
	參與計畫人力（外國籍）	碩士生	0	0	100%	人次	
		博士生	0	0	100%		
		博士後研究員	0	0	100%		
		專任助理	0	0	100%		

其他成果 (無法以量化表達之成果如辦理學術活動、獲得獎項、重要國際合作、研究成果國際影響力及其他協助產業技術發展之具體效益事項等，請以文字敘述填列。)	1.可利用之產業及可開發之產品:建築營造、房地產、節能省能及能源科技業 建築物帷幕系統、建築物節能省能系統規畫 綠建築混成設計最佳化軟體. 2.技術特點: 綠建築 節能省能 能源材料 環保 氣電熱整合. 3.推廣及運用的價值: Green Housing Shape-stabilized Phase Change Materials Save Energy and Protect Environment 4. Section Chair--WSEAS/NAUN International Conferences: 2nd International Conference on Fluid Mechanics and Heat and Mass Transfer 2011 (FLUIDSHEAT'11), Corfu Island, Greece., July 2011.

	成果項目	量化	名稱或內容性質簡述
科教處計畫加填項目	測驗工具(含質性與量性)	0	
	課程/模組	0	
	電腦及網路系統或工具	0	
	教材	0	
	舉辦之活動/競賽	0	
	研討會/工作坊	0	
	電子報、網站	0	
	計畫成果推廣之參與（閱聽）人數	0	

國科會補助專題研究計畫成果報告自評表

請就研究內容與原計畫相符程度、達成預期目標情況、研究成果之學術或應用價值（簡要敘述成果所代表之意義、價值、影響或進一步發展之可能性）、是否適合在學術期刊發表或申請專利、主要發現或其他有關價值等，作一綜合評估。

1. 請就研究內容與原計畫相符程度、達成預期目標情況作一綜合評估

■達成目標

□未達成目標（請說明，以 100 字為限）

□實驗失敗

□因故實驗中斷

□其他原因

說明：

2. 研究成果在學術期刊發表或申請專利等情形：

論文：■已發表 □未發表之文稿 □撰寫中 □無

專利：□已獲得 □申請中 ■無

技轉：□已技轉 ■洽談中 □無

其他：（以 100 字為限）

論文

國際期刊論文有 3 篇:

1. Advanced Material Research (EI) 2. Advanced Science Letters (SCI) 3. International J. of Energy (SCI EI)

國際期刊有 1 篇: 審查中

WSEAS Trans. J. (SCI)

國外研討會有 5 篇 國內有 1 篇、碩士論文有一

專利

實體雛型之實驗數據驗證再作專利申請

技術移轉

洽談中:喜室(Hess energy Co.) 台灣寶熊

3. 請依學術成就、技術創新、社會影響等方面，評估研究成果之學術或應用價值（簡要敘述成果所代表之意義、價值、影響或進一步發展之可能性）（以 500 字為限）

建築物越來越注重本身自己就是節能減碳有效率，因此自然通風、太陽能加溫與致冷、地溫空氣熱交換、自然光線及避陽遮蔭…等自然被動式不需要消耗太多能量的設置，將是綠色建築的不二選擇，本研究三機一體將薄膜光伏電熱太陽能板空氣收集器(PV/T air collector), 收集熱氣驅動氣流、搭配地溫空氣熱交換(EAHE)來的氣流與吸收透過窗戶或太陽能板光線的穩態形狀相變材料(SSPCM)之儲熱儲能，整合出一棟完全被動式混成系統建築。考慮新材料與建築服務結合的綠色設計新觀念，再以一棟位於台灣新竹地區沒有空調的建物為探討對象，來數值分析仲夏夜晚通風情況下，氣、電及熱的需求與影響，分析時程含蓋日、月及年，先針對薄膜光伏電熱太陽能板與各次系統之物理數學模型(Model)驗證，再發展出被動式混成系統建築的完整物理數學模型，搭配 MATHLAB、CFD 軟體協助

而得到分析解及數值解。

利用熵值公式(enthalpy formulation)及 Voller 與 Patankar 之控制容積數值技術求解二維暫態能量守恆搭配 Stefan 移動邊界問題幅與波數下，自然對流具有最佳的熱傳增益。之福傳程式組 Hybrid-HVAC，也將配合本棟被動式混成系統建築的個別次系統做程式修改為 Hybrid-HVACP，此程式可以幫忙材料作驗證，以及協助太陽能電池空氣收集器、地溫空氣熱交換及穩態形狀相變材料地板等系統作設計，為綠色建築-節能省能屋的最佳化設計與能量分析，提供有利的工具。

可利用之產業及可開發之產品：建築營造、房地產、節能省能及能源科技業。

建築物帷幕系統、建築物節能省能系統規畫 綠建築混成設計最佳化軟體

技術特點：綠建築 節能省能 能源材料 環保 氣電熱整合